REPORT

DNA Polymerase Epsilon Deficiency Causes IMAGe Syndrome with Variable Immunodeficiency

Clare V. Logan,[1,32] Jennie E. Murray,[1,2,32,*] David A. Parry,[1] Andrea Robertson,[1] Roberto Bellelli,[3] Žygimantė Tarnauskaitė,[1] Rachel Challis,[1,2] Louise Cleal,[1,2] Valerie Borel,[3] Adeline Fluteau,[1] Javier Santoyo-Lopez,[4] SGP Consortium, Tim Aitman,[5] Inês Barroso,[6] Donald Basel,[7] Louise S. Bicknell,[8] Himanshu Goel,[9,10] Hao Hu,[11] Chad Huff,[11] Michele Hutchison,[12] Caroline Joyce,[13] Rachel Knox,[14] Amy E. Lacroix,[15] Sylvie Langlois,[16] Shawn McCandless,[17] Julie McCarrier,[7] Kay A. Metcalfe,[18] Rose Morrissey,[19] Nuala Murphy,[20] Irène Netchine,[21] Susan M. O'Connell,[20] Ann Haskins Olney,[15] Nandina Paria,[22] Jill A. Rosenfeld,[23] Mark Sherlock,[24] Erin Syverson,[7] Perrin C. White,[25] Carol Wise,[22,25,26,27] Yao Yu,[11] Margaret Zacharin,[28] Indraneel Banerjee,[29] Martin Reijns,[1] Michael B. Bober,[30] Robert K. Semple,[14,31] Simon J. Boulton,[3] Jonathan J. Rios,[22,25,26,27] and Andrew P. Jackson[1,*]

During genome replication, polymerase epsilon (Pol ε) acts as the major leading-strand DNA polymerase. Here we report the identification of biallelic mutations in *POLE*, encoding the Pol ε catalytic subunit POLE1, in 15 individuals from 12 families. Phenotypically, these individuals had clinical features closely resembling IMAGe syndrome (intrauterine growth restriction [IUGR], metaphyseal dysplasia, adrenal hypoplasia congenita, and genitourinary anomalies in males), a disorder previously associated with gain-of-function mutations in *CDKN1C*. POLE1-deficient individuals also exhibited distinctive facial features and variable immune dysfunction with evidence of lymphocyte deficiency. All subjects shared the same intronic variant (c.1686+32C>G) as part of a common haplotype, in combination with different loss-of-function variants in *trans*. The intronic variant alters splicing, and together the biallelic mutations lead to cellular deficiency of Pol ε and delayed S-phase progression. In summary, we establish *POLE* as a second gene in which mutations cause IMAGe syndrome. These findings add to a growing list of disorders due to mutations in DNA replication genes that manifest growth restriction alongside adrenal dysfunction and/or immunodeficiency, consolidating these as replisome phenotypes and highlighting a need for future studies to understand the tissue-specific development roles of the encoded proteins.

DNA replication is a fundamental cellular process necessary to ensure the faithful transmission of genetic information. In eukaryotes, three highly conserved DNA polymerases, polymerase epsilon, delta, and alpha, act in concert at the replication fork. Polymerase epsilon (Pol ε) is the major enzyme responsible for the synthesis of the leading strand[1] and is consequently an essential gene.[2] *POLE* encodes the catalytic subunit of Pol ε (POLE1), and somatic and germline missense mutations affecting the proofreading domain of POLE1 have been associated with colon and endometrial cancer.[3–6]

Microcephalic primordial dwarfism comprises a group of prenatal-onset extreme growth disorders characterized by intrauterine growth retardation, short stature, and microcephaly. Genes involved in cell cycle progression, including multiple components of the replication licensing machinery, have been identified as monogenic causes of this disorder.[7–11] As the molecular basis for many affected individuals remains to be determined, we performed whole-genome sequencing studies to identify further genes and facilitate more comprehensive diagnosis.

[1]MRC Human Genetics Unit, MRC Institute of Genetics and Molecular Medicine, University of Edinburgh, Edinburgh EH4 2XU, UK; [2]South East Scotland Clinical Genetics Service, Western General Hospital, Edinburgh EH4 2XU, UK; [3]The Francis Crick Institute, 1 Midland Road, London NW1 1AT, UK; [4]Edinburgh Genomics Clinical Division, University of Edinburgh, The Roslin Institute, Edinburgh EH25 9RG, UK; [5]MRC Centre for Genomic & Experimental Medicine, MRC Institute of Genetics and Molecular Medicine, University of Edinburgh, Edinburgh EH4 2XU, UK; [6]Wellcome Sanger Institute, Cambridge CB10 1SA, UK; [7]Medical College of Wisconsin from Children's Hospital of Wisconsin, Milwaukee, WI 53226, USA; [8]Department of Pathology, Dunedin School of Medicine, University of Otago, Dunedin 9016, New Zealand; [9]Hunter Genetics, Waratah, NSW 2305, Australia; [10]University of Newcastle, Callaghan, NSW 2308, Australia; [11]Department of Epidemiology, MD Anderson Cancer Center, Houston, TX 77030, USA; [12]Department of Pediatrics, University of Arkansas, Little Rock, AR 72205, USA; [13]Department of Clinical Biochemistry, Cork University Hospital, Cork, Ireland; [14]MRC Metabolic Diseases Unit, University of Cambridge, Cambridge CB2 0QQ, UK; [15]University of Nebraska Medical Centre, Omaha, NE 68918, USA; [16]Department of Medical Genetics, The University of British Columbia, Vancouver, BC V6H 3N1, Canada; [17]Pediatric Genetics, UH Cleveland Medical Center, Cleveland, OH 44106, USA; [18]Manchester Centre for Genomic Medicine, Manchester University NHS Foundation Trust and Institute of Human Development, University of Manchester, Manchester M13 9WL, UK; [19]Department of Paediatrics and Child Health, Cork University Hospital, Cork, Ireland; [20]UCD School of Medicine, Children's University Hospital, Temple St, Dublin, Ireland; [21]Sorbonne Université, INSERM, UMR_S 938, APHP, Hospital Trousseau, 75012 Paris, France; [22]Sarah M. and Charles E. Seay Center for Musculoskeletal Research, Texas Scottish Rite Hospital for Children, Dallas, TX 75219, USA; [23]Department of Molecular and Human Genetics, Baylor College of Medicine, Houston, TX 77030, USA; [24]Department of Endocrinology, Beaumont Hospital, Dublin, Ireland; [25]Department of Pediatrics, University of Texas Southwestern Medical Center, Dallas, TX 75390, USA; [26]Department of Orthopaedic Surgery, University of Texas Southwestern Medical Center, Dallas, TX 75390, USA; [27]McDermott Center for Human Growth and Development, University of Texas Southwestern Medical Center, Dallas, TX 75390, USA; [28]Division of Medicine, Royal Children's Hospital, Melbourne, VIC 3052, Australia; [29]Department of Paediatric Endocrinology, Royal Manchester Children's Hospital, Manchester Academic Health Science Centre, Manchester M13 9WU, UK; [30]Nemours-Alfred I. duPont Hospital for Children, Wilmington, DE 19803, USA; [31]Centre for Cardiovascular Science, University of Edinburgh, Edinburgh EH16 4TJ, UK

[32]These authors contributed equally to this work

*Correspondence: jennie.murray@igmm.ed.ac.uk (J.E.M.), andrew.jackson@igmm.ed.ac.uk (A.P.J.)

https://doi.org/10.1016/j.ajhg.2018.10.024.

Table 1. Biallelic *POLE* Mutations (GenBank: NM_006231.3)

			Allele 1			Allele 2					
ID	Fam	Sex	Nucleotide Change	Amino Acid Consequence	MAF	Nucleotide Change	Amino Acid Consequence	MAF	Mat Allele	Pat Allele	Country of Origin
P1	1	M	c.2091dupC	p.Phe699Valfs*11	0	c.1686+32C>G	p.Asn563Valfs*16	0.000071	1	2	UK
P2	1	F	c.2091dupC	p.Phe699Valfs*11	0	c.1686+32C>G	p.Asn563Valfs*16	0.000071	1	2	UK
P3	2	M	c.62+1G>A	Essential Splice Site Intron 1	0	c.1686+32C>G	p.Asn563Valfs*16	0.000071	2	1	Ireland
P4	3	F	c.5940G>A	p.Trp1980*	0.000016	c.1686+32C>G	p.Asn563Valfs*16	0.000071	2	1	Australia
P5	4	M	c.4728+1G>T	Essential Splice Site Intron 36	0	c.1686+32C>G	p.Asn563Valfs*16	0.000071	2	1	USA
P6	5	F	c.3264_3275+13del	Essential Splice Site Intron 26	0.000016	c.1686+32C>G	p.Asn563Valfs*16	0.000071	1	2	Canada
P7	6	M	c.1A>T	p.?	0.000081	c.1686+32C>G	p.Asn563Valfs*16	0.000071	n/a	n/a	USA
P8	7	M	c.1A>T	p.?	0.000081	c.1686+32C>G	p.Asn563Valfs*16	0.000071	2	1	Ireland
P9	7	F	c.1A>T	p.?	0.000081	c.1686+32C>G	p.Asn563Valfs*16	0.000071	2	1	Ireland
P10	8	F	c.3019G>C	p.Ala1007Pro	0.000009	c.1686+32C>G	p.Asn563Valfs*16	0.000071	1	2	Ireland
P11	9	F	c.5265delG	Ile1756Serfs*5	0	c.1686+32C>G	p.Asn563Valfs*16	0.000071	2	1	Australia
P12	9	M	c.5265delG	Ile1756Serfs*5	0	c.1686+32C>G	p.Asn563Valfs*16	0.000071	2	1	Australia
P13	10	F	c.2049C>G	p.Tyr683*	0.000028	c.1686+32C>G	p.Asn563Valfs*16	0.000071	1	2	Australia
P14	11	M	c.6518_6519delCT	p.Ser2173Phefs*130	0.000089	c.1686+32C>G	p.Asn563Valfs*16	0.000071	2	1	USA
P15	12	M	c.801+2T>C	Essential Splice Site Intron 8	–	c.1686+32C>G	p.Asn563Valfs*16	0.000071	1	2	USA

Abbreviations: ID, individual number; Fam, family number; Mat, maternal; Pat, paternal; n/a, not available. All subjects harbored a loss-of-function mutation in combination with an intronic variant on the alternate allele identified as part of a shared haplotype and found to alter splicing in RNA studies. MAF indicates minor allele frequency in European (non-Finnish) population observed in gnomAD. None of the variants were present in any Non-European population in gnomAD.

Whole-genome sequencing (WGS) of 48 individuals with microcephalic primordial dwarfism identified heterozygous *POLE* (GenBank: NM_006231.3) loss-of-function (LoF) variants in three subjects (P1, P3, P4; Table 1). These LoF variants were significantly enriched in our cohort compared to a control WGS dataset (GnomAD,[12] $p = 5.1 \times 10^{-5}$, Fisher's exact test, Table S1). As these variants were present in the unaffected parents, the WGS data were further evaluated and a second rare intronic variant in *POLE* identified, c.1686+32C>G (dbSNP: rs762985435). This was present in *trans* with the LoF mutation in all three probands (Table 1). Targeted sequencing of *POLE* and interrogation of existing whole-exome sequencing (WES) data in additional cases of primordial dwarfism identified five additional subjects compound heterozygous for LoF alleles and the c.1686+32C>G variant (P5–P9, Table 1). Notably, a clinical diagnosis of IMAGe syndrome (GeneReviews in Web Resources) (MIM: 614732) had been considered in individuals P1 and P3, with adrenal failure also reported in P5, P6, and P7. We therefore investigated cases of IMAGe syndrome drawn from other cohorts without an existing molecular diagnosis (i.e., *CDKN1C* mutation negative). These included three previously published IMAGe-affected case subjects.[13,14] Analysis of their WGS data identified additional *POLE* LoF variants inherited in *trans* with the intronic variant in individuals P11–P15 (Table 1). The c.1686+32C>G variant was part of a common haplotype in all individuals where WES/WGS performed, extending over 921 kbp (Figure S2, chr12:132341818–133263107, GRCh38). In P10 a missense variant (c.3019G>C) encoding a p.Ala1007Pro substitution was found, at a residue conserved to yeast (Figure S1) within the polymerase domain of the protein (Figure 1). All variants identified were sufficiently rare (MAF < 0.0001[12]) and, where DNA available, segregation in families was consistent with an autosomal recessively inherited disorder (Table 1).

Phenotypically, affected individuals had severe growth failure of prenatal onset (Figure 2, Table S2). IUGR was present in all case subjects (birth weight was −3.0 ± 0.8 SD) with significant short stature evident postnatally (height −8.1 ± 2.4 SD). While head circumference was also significantly reduced (OFC −5.4 ± 1.5 SD), this was less severe, resulting in a relative macrocephaly. Those affected had a common facial appearance with micrognathia, crowded dentition, long thin nose, short wide neck, and small, low-set, posteriorly rotated ears (Figure 2). 12 individuals had adrenal insufficiency and all affected males had genitourinary abnormalities including bilateral cryptorchidism and/or hypospadias, with the majority of case subjects fulfilling clinical criteria for IMAGe syndrome (GeneReviews in Web Resources; Table 2, Table S3, Supplemental Note).

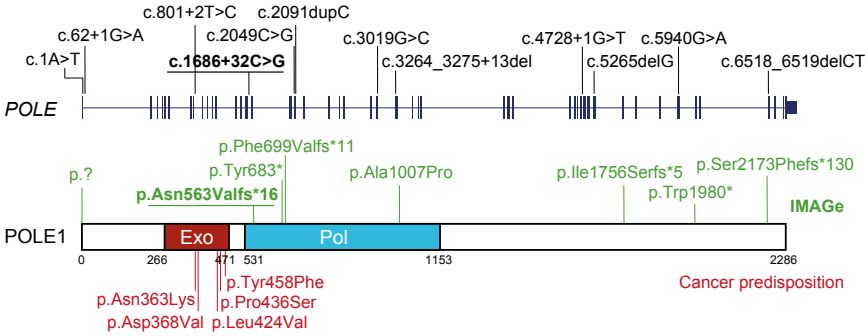

Figure 1. Mutations Causing *POLE*-Associated IMAGe Syndrome Are Distinct from Mutations Conferring a Non-syndromic Susceptibility to Cancer
Schematic of the *POLE* gene, which encodes POLE1, the catalytic subunit of DNA polymerase epsilon. Domains: Pol, polymerase; Exo, exonuclease. Mutations identified in *POLE* subjects indicated above gene and protein (green). Recurrent intronic mutation underlined. For comparison, heterozygous germline missense mutations located in the exonuclease domain predisposing to colorectal cancer and other malignancies highlighted below (red).

Osteopenia and developmental dysplasia of the hip (DDH) were frequently observed and café-au-lait patches were notably present in a third of individuals.

A single homozygous intronic variant (c.4444+3A>G) in *POLE* has previously been reported to be associated with immunodeficiency, lymphopenia, and short stature (facial dysmorphism, immunodeficiency, livedo, and short stature, aka FILS syndrome [MIM: 615139]).[15,16] Five affected individuals identified in this study also had increased susceptibility to respiratory tract infections, with lymphocyte subset deficiencies and/or IgM hypogammaglobinemia identified in P1, P3, P4, P8, P9, P14, and P15 (Table 2, Table S4). Deficiency of natural killer cells was present in P1, P3, and P8. P1 had the most profound immunodeficiency, developing CMV pneumonitis and then subsequently developed EBV haemophagocytic lymphohistiocytosis, requiring an allogeneic bone marrow transplant. Notably, this subject's sister (P2), who had the same compound heterozygous *POLE* mutations, died at 22 months from HSV infection. Therefore, our findings establish that the phenotype spectrum of biallelic *POLE* mutations extends from IMAGe syndrome to include immunodeficiency, in line with the phenotype and pathogenicity of the previously reported c.4444+3A>G mutation.[15,16]

To establish whether the c.1686+32C>T variant affected the *POLE* transcript, RNA studies were performed on primary fibroblast lines derived from two subjects (P1, P3). RT-PCR using primers spanning *POLE* intron 15 demonstrated the presence of a larger PCR product (Figure 3), which capillary sequencing established to be due to retention of part of intron 15 within *POLE* transcripts (Figure S3). A minigene assay was then performed to assess splicing of this genomic segment and to directly confirm the contribution of the c.1686+32C>G variant. This demonstrated that the c.1686+32C>G variant markedly impaired splicing of the usual exon 15 splice donor site, leading to preferential use of a downstream alternate splice donor site in intron 15, although some canonical splicing also occurred (Figure 3). The inclusion of 47 bp of intronic

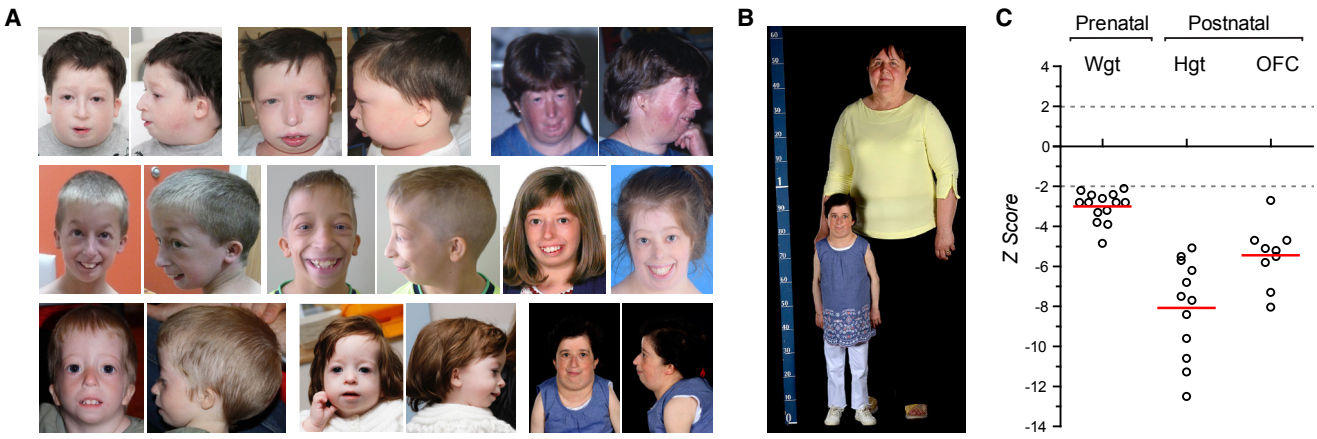

Figure 2. Individuals with Biallelic *POLE* Mutations Have Severely Impaired Pre- and Post-natal Growth and a Recognizable Facial Gestalt
(A) Photographs of *POLE*-deficient subjects demonstrating facial similarities. Written consent obtained from all families for photography.
(B and C) Severe pre-natal onset growth restriction occurs in *POLE*-deficient individuals.
(B) Adult *POLE*-deficient subject next to a control individual of average stature.
(C) Growth is severely impaired pre- and postnatally. Z-scores (standard deviations from population mean for age and sex) for birth weight and postnatal height and head circumference (OFC). Dashed lines 95% confidence interval for general population. Circles, individual subject data points; red bars, mean values.

Table 2. Individuals with Biallelic Mutations in *POLE* Were Clinically Diagnosed with Primordial Dwarfism and Features of IMAGe Syndrome

ID	Fam	Sex	Age	I	M_{+SI}	A	Ge	−I	Other Features
P1	1	M	18	Y	Y	Y	Y	Y	scoliosis, osteopenia, small patella, seizures, gastrostomy, eczema
P2	1	F	1	Y	Y	Y	–	Y	–
P3	2	M	7	Y	Y	Y	Y	Y	midline accessory incisor, osteopenia, infant eczema
P4	3	F	50	Y	Y	N	–	Y	IgM paraproteinaemia
P5	4	M	12	Y	NA	Y	Y	Y	hypopituitarism, T cell lymphoma, gastrostomy, absent patella
P6	5	F	10	Y	Y	Y	–	Y	bilat coxa valga, 11 ribs, 6 lumbar vertebrae, scoliosis, gastrostomy, infant eczema
P7	6	M	13	Y	Y	Y	Y	N	hypopituitarism, atrial septal defect, brachydactyly, gastrostomy
P8	7	M	3	Y	Y	N	Y	Y	DDH, gastrostomy
P9	7	F	2	Y	Y	N	–	Y	DDH, gastrostomy
P10	8	F	39	Y	Y	Y	–	N	DDH, 11 ribs, clinodactyly, osteopenia, café au lait patches
P11	9	F	0.2	Y	NA	Y	–	Y	café au lait patch
P12	9	F	12	Y	Y	Y	–	N	–
P13	10	M	22	Y	Y	Y	Y	N	DDH, café au lait patch
P14	11	F	18	Y	Y	Y	–	Y	gastrostomy, hypercalaemia in infancy, café au lait patches, DDH, kyphoscoliosis
P15	12	M	31	Y	NA	Y	Y	Y	café au lait patches, seizures, osteopenia, osteoporosis, nodular sclerosis, Hodgkin's lymphoma

Abbreviations: ID, individual number; Fam, family number; I, intrauterine growth restriction; M_{+SI}, skeletal involvement: metaphyseal dysplasia or other skeletal abnormalities reported in CDKN1C IMAGe-affected individuals (NA, not assessed); A, adrenal insufficiency; Ge, genitourinary abnormalities in males (– female, genitourinary anomalies not applicable); −I, immunodeficiency, either increased susceptibility to infections or documented lymphopenia/hypogammaglobinemia; DDH, developmental dysplasia of the hip; Y, yes; N, no. See Tables S1–S4 for extended clinical data and morphometrics.

DNA in the variant transcript results in a frameshift, which would lead to premature termination (p.Asn563Valfs*16). While this transcript might be targeted for nonsense-mediated decay, any translated protein would also be non-functional given that this frameshift occurs at the start of the polymerase catalytic domain. Combined with a LoF mutation on the second allele, substantial reduction in POLE1 was therefore anticipated. Subsequent immunoblotting of total protein extracts from of primary fibroblasts from affected subjects confirmed that POLE1 levels were indeed markedly depleted (Figure 3; 5% ± 3% for P1 and 11% ± 4% P3, relative to the mean of both control subjects and normalized to vinculin loading control; mean ± SD for n = 2 independent experiments), with chromatin fractionation experiments demonstrating reduction of POLE1 in both soluble and chromatin-bound fractions (Figure S4). Taken together with the consistent clinical phenotype across case subjects, we concluded that the identified *POLE* variants were pathogenic, resulting in a phenotype spectrum substantially overlapping IMAGe syndrome.

In keeping with an essential requirement for *POLE* in eukaryotes,[2] the "leaky" c.1686+32C>G splice mutation permitted residual expression of functional POLE1 in all case subjects. This mutation in *trans* with truncating mutations would then be expected to lead to marked but partial loss of function. As *POLE* encodes POLE1, the catalytic subunit of the major leading-strand DNA polymerase Pol ε, reduced chromatin levels of POLE1 would therefore be expected to impact on the availability of Pol ε DNA polymerase activity during its canonical function in DNA replication. Consistent with this, time-course FACS analysis demonstrated delayed cell-cycle progression of BrdU-labeled primary fibroblasts from P1 and P3, indicative of impaired S-phase progression (Figure 3). While no viable model of POLE1 deficiency exists, a *Pole4*$^{-/-}$ mouse has been generated, which is similarly deficient for the Pol ε holoenzyme.[17] This mouse also has significant prenatal onset growth failure, reduced brain size, and markedly reduced lymphocyte levels. Analysis of embryonic fibroblasts derived from this mouse alongside *POLE* primary human fibroblasts (derived from P1 and P3 in this study) established that in both cases Pol ε deficiency leads to reduced levels of chromatin-loaded Pol ε complexes, resulting in replication stress arising from reduced numbers of active replication origins.[17]

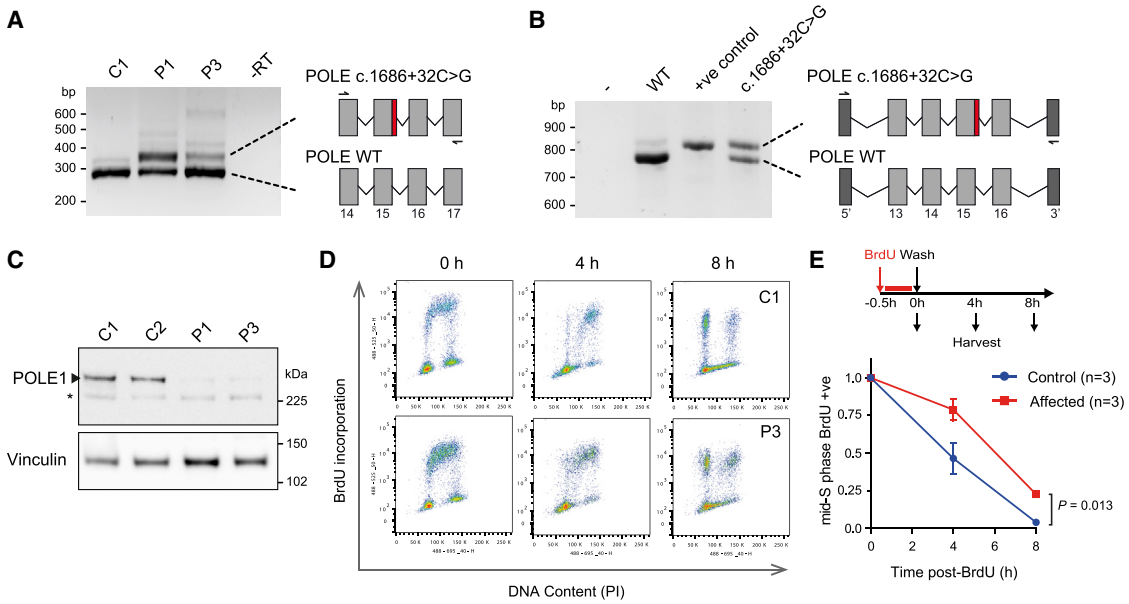

Figure 3. Common Intronic Variant Identified Causes Aberrant Splicing and *POLE*-Deficient Cells Show Deficiency of Polymerase Epsilon and Slowed S-phase Progression

(A) The c.1686+32C>G mutation causes aberrant splicing of intron 15 in subject cells. RT-PCR of *POLE* transcripts from primary fibroblasts. Primers indicated by arrows in schematic. P1, P3, POLE-deficient subjects; C1, C2, control subjects.

(B) Minigene assay demonstrating that aberrant splicing is a direct consequence of the c.1686+32C>G mutation. +ve control, point mutation in splice donor site, c.1686+1G>A. 5′ & 3′ indicate artificial vector-associated exons.

(C) POLE1 levels are markedly reduced in subject fibroblasts. Immunoblot of total cell extracts. POLE1 antibody raised against AA1-176. Vinculin, loading control. * non-specific band.

(D and E) Fibroblast cells from affected individuals exhibit delayed S phase progression. Schematic, experimental set-up.

(D) Representative FACS plots.

(E) Quantification of n = 3 affected and n = 3 control cell lines from representative experiment (of n = 3 expts with n ≥ 2 biological replicates per group). Mid-S-phase mean (±SEM) BrdU-labeled cells, normalized to t = 0 time point are plotted for each group. p value, two-way ANOVA.

IMAGe syndrome has previously been found to be caused by dominant gain-of-function mutations in the imprinted gene, *CDKN1C*.[18,19] Here, we establish mutations of *POLE* as an autosomal-recessive cause of the IMAGe phenotype. These mutations contrast with heterozygous germline and somatic cancer-predisposing mutations that affect the exonuclease domain of POLE1[3–6] (Figure 1). IMAGe and cancer mutations are likely to have differing functional outcomes, respectively leading to deficient DNA replication or to impaired proof-reading.[20] Hence, a similar cancer predisposition in POLE1-deficient individuals or POLE heterozygous carriers cannot be assumed. However, P5 developed a T cell lymphoma at age 11 and P15 developed Hodgkin's lymphoma at age 28. Given also the increased lymphoma rates in *Pole4*$^{-/-}$ mice,[17] POLE1 deficiency may therefore confer an increased risk of lymphoma.

All *CDKN1C* IMAGe mutations cluster within its proliferating cell nuclear antigen (PCNA) binding domain,[18,19] targeting the PCNA binding PIP-box motif.[21] As PCNA loads with Pol ε at replication initiation (Figures 4 and S5), the phenotypic overlap with *POLE*-associated IMAGe syndrome suggests a mechanistic link. Supporting this notion, biochemical studies of a *Xenopus* homolog suggests that CDKN ubiquitination and subsequent degradation is mediated by PCNA/polymerase loading[23,24] (Figure S5). Furthermore, single homozygous mutations in *MCM4*[11,25] (MIM: 609981) and *POLE2*[26] have been associated with IUGR and short stature, alongside immunodeficiency, respectively with and without adrenal failure. Likewise, several families with *GINS1* biallelic mutations have been reported to be associated with pre/postnatal growth restriction, chronic neutropenia, and NK cell deficiency (MIM: 610608).[10] Hence, the identification of a cohort of individuals with *POLE* mutations that encompasses all these features consolidates this as a group of replisome-associated disorders (Figure 4, Table S5). Replication stress and p53-mediated cell death[17] likely explain the immunodeficiency as well as global growth failure in POLE1-deficient individuals. However, why impaired replisome function should have a particularly strong impact on specific lymphoid lineages (T/B cells in POLE1/2-deficient subjects and NK cells in MCM4/GINS1-deficient individuals) or on adrenal cortical cells is unclear. Notably, another distinct form of primordial dwarfism, Meier-Gorlin syndrome (defined by the triad of short stature, patella hypoplasia, and microtia [MIM: 224690]) is also caused by biallelic (or *de novo*) mutations in genes involved in replication licensing and initiation[7–9,27,28] (Figure 4). Further studies to understand the specific role(s) of the encoded

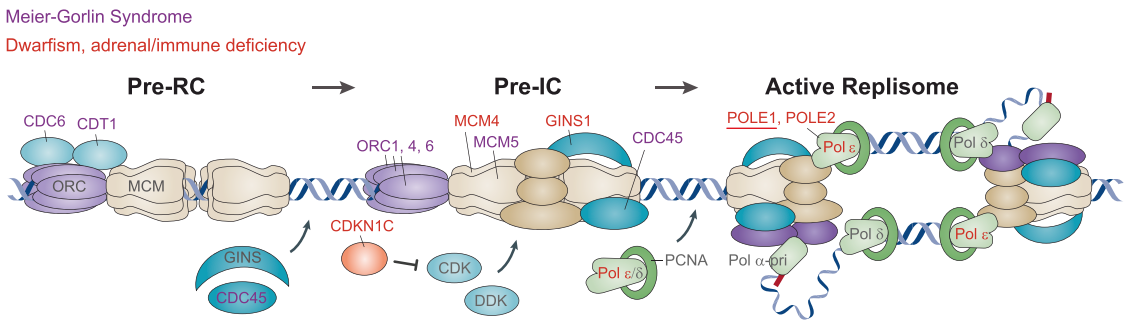

Figure 4. POLE1 Deficiency Links *CDKN1C*-IMAGe Syndrome[18] with Other Replisome-Associated Disorders
Schematic of replication initiation (adapted by permission from Gaillard et al.[22] copyright 2015 Macmillan Publishers), highlighting the sequential action of replisome-associated proteins, mutation of which causes MGS (blue text) and those that are associated with dwarfism with adrenal insufficiency and/or immune deficiency, including IMAGe syndrome (red text). During replication licensing, MCM helicases (MCM2-7) are loaded at replication origins by the ORC complex (ORC1-6) with CDC6 and CDT1 to form the pre-replicative complex (pre-RC). Subsequently, loading of additional replisome protein occurs, regulated by DDK and CDK kinases, to form the pre-initiation complex (pre-IC), that contains the CMG (CDC45, MCMs, GINS) complex. CDKN1C inhibits CDK activity. In the active replisome, Primase-Pol α initiates DNA synthesis with strands extended by the PCNA-associated DNA polymerases δ and ε. POLE1 and POLE2 are part of the Pol ε holoenzyme.

replication proteins during development, along with the cellular and biochemical basis for the relationship between CDKN1C and Pol ε, will therefore be of interest.

Supplemental Data

Supplemental Data include Supplemental Note, seven figures, five tables, and Supplemental Material and Methods and can be found with this article online at https://doi.org/10.1016/j.ajhg.2018.10.024.

Consortia

Members of the Scottish Genome Partnership include Timothy J. Aitman, Andrew V. Biankin, Susanna L. Cooke, Wendy Inglis Humphrey, Sancha Martin, Lynne Mennie, Alison Meynert, Zosia Miedzybrodzka, Fiona Murphy, Craig Nourse, Javier Santoyo-Lopez, Colin A. Semple, and Nicola Williams.

Acknowledgments

We thank the families and clinicians for their involvement and participation; the Potentials Foundation and Walking with Giants Foundation; D. Fitzpatrick, N. Hastie, and W. Bickmore for discussions; E. Freyer for assistance with FACS analysis; IGMM core sequencing service; and Edinburgh Genomics (Clinical Division) for WGS sequencing. We thank Penny Jeggo for sharing cell lines. This work was supported by funding to the Jackson lab from European Research Council ERC Starter Grant HumGenSize, 281847; ERC Advanced Investigator Grant GrowCell, 788093; by a UK Medical Research Council Human Genetics Unit core grant (MRC, U127580972), and the Scottish Genomes Partnership. The Rios lab is supported by Texas Scottish Rite Hospital for Children and the Children's Medical Center Foundation. Research reported in this publication was supported by the National Center for Advancing Translational Sciences of the National Institutes of Health under award number UL1TR001105. The content is solely the responsibility of the authors and does not necessarily represent the official views of the NIH. Boulton lab work is supported by the Francis Crick Institute, which receives its core funding from Cancer Research UK (FC0010048), the UK Medical Research Council (FC0010048), and the Wellcome Trust (FC0010048); a European Research Council (ERC) Advanced Investigator Grant (TelMetab); and Wellcome Trust Senior Investigator and Collaborative Grants. R.K.S. is funded by the Wellcome Trust (210752/Z/18/Z). The Scottish Genomes Partnership is funded by the Chief Scientist Office of the Scottish Government Health Directorates (SGP/1) and The Medical Research Council Whole Genome Sequencing for Health and Wealth Initiative.

Declaration of Interests

The Department of Molecular and Human Genetics at Baylor College of Medicine receives revenue from the genetic testing services offered by Baylor Genetics.

Received: August 6, 2018
Accepted: October 26, 2018
Published: November 29, 2018

Web Resources

dbSNP, https://www.ncbi.nlm.nih.gov/projects/SNP/
GenBank, https://www.ncbi.nlm.nih.gov/genbank/
GeneReviews, Bennett, J., Schrier Vergano, S.A., and Deardorff, M.A. (1993). IMAGe syndrome, https://www.ncbi.nlm.nih.gov/books/NBK190103/
gnomAD Browser, http://gnomad.broadinstitute.org/
OMIM, http://www.omim.org/

References

1. Burgers, P.M.J., and Kunkel, T.A. (2017). Eukaryotic DNA replication fork. Annu. Rev. Biochem. *86*, 417–438.
2. Hogg, M., and Johansson, E. (2012). DNA polymerase ε. Subcell. Biochem. *62*, 237–257.
3. Palles, C., Cazier, J.B., Howarth, K.M., Domingo, E., Jones, A.M., Broderick, P., Kemp, Z., Spain, S.L., Guarino, E., Salguero, I., et al.; CORGI Consortium; and WGS500 Consortium (2013). Germline mutations affecting the proofreading

domains of POLE and POLD1 predispose to colorectal adenomas and carcinomas. Nat. Genet. *45*, 136–144.
4. Church, D.N., Briggs, S.E., Palles, C., Domingo, E., Kearsey, S.J., Grimes, J.M., Gorman, M., Martin, L., Howarth, K.M., Hodgson, S.V., et al.; NSECG Collaborators (2013). DNA polymerase ε and δ exonuclease domain mutations in endometrial cancer. Hum. Mol. Genet. *22*, 2820–2828.
5. Bellido, F., Pineda, M., Aiza, G., Valdés-Mas, R., Navarro, M., Puente, D.A., Pons, T., González, S., Iglesias, S., Darder, E., et al. (2016). POLE and POLD1 mutations in 529 kindred with familial colorectal cancer and/or polyposis: review of reported cases and recommendations for genetic testing and surveillance. Genet. Med. *18*, 325–332.
6. Cancer Genome Atlas, N.; and Cancer Genome Atlas Network (2012). Comprehensive molecular characterization of human colon and rectal cancer. Nature *487*, 330–337.
7. Bicknell, L.S., Bongers, E.M., Leitch, A., Brown, S., Schoots, J., Harley, M.E., Aftimos, S., Al-Aama, J.Y., Bober, M., Brown, P.A., et al. (2011). Mutations in the pre-replication complex cause Meier-Gorlin syndrome. Nat. Genet. *43*, 356–359.
8. Bicknell, L.S., Walker, S., Klingseisen, A., Stiff, T., Leitch, A., Kerzendorfer, C., Martin, C.A., Yeyati, P., Al Sanna, N., Bober, M., et al. (2011). Mutations in ORC1, encoding the largest subunit of the origin recognition complex, cause microcephalic primordial dwarfism resembling Meier-Gorlin syndrome. Nat. Genet. *43*, 350–355.
9. Fenwick, A.L., Kliszczak, M., Cooper, F., Murray, J., Sanchez-Pulido, L., Twigg, S.R.F., Goriely, A., McGowan, S.J., Miller, K.A., Taylor, I.B., et al.; WGS500 Consortium (2016). Mutations in CDC45, Encoding an Essential Component of the Pre-initiation Complex, Cause Meier-Gorlin Syndrome and Craniosynostosis. Am. J. Hum. Genet. *99*, 125–138.
10. Cottineau, J., Kottemann, M.C., Lach, F.P., Kang, Y.H., Vély, F., Deenick, E.K., Lazarov, T., Gineau, L., Wang, Y., Farina, A., et al. (2017). Inherited GINS1 deficiency underlies growth retardation along with neutropenia and NK cell deficiency. J. Clin. Invest. *127*, 1991–2006.
11. Gineau, L., Cognet, C., Kara, N., Lach, F.P., Dunne, J., Veturi, U., Picard, C., Trouillet, C., Eidenschenk, C., Aoufouchi, S., et al. (2012). Partial MCM4 deficiency in patients with growth retardation, adrenal insufficiency, and natural killer cell deficiency. J. Clin. Invest. *122*, 821–832.
12. Lek, M., Karczewski, K.J., Minikel, E.V., Samocha, K.E., Banks, E., Fennell, T., O'Donnell-Luria, A.H., Ware, J.S., Hill, A.J., Cummings, B.B., et al.; Exome Aggregation Consortium (2016). Analysis of protein-coding genetic variation in 60,706 humans. Nature *536*, 285–291.
13. Tan, T.Y., Jameson, J.L., Campbell, P.E., Ekert, P.G., Zacharin, M., and Savarirayan, R. (2006). Two sisters with IMAGe syndrome: cytomegalic adrenal histopathology, support for autosomal recessive inheritance and literature review. Am. J. Med. Genet. A. *140*, 1778–1784.
14. Pedreira, C.C., Savarirayan, R., and Zacharin, M.R. (2004). IMAGe syndrome: a complex disorder affecting growth, adrenal and gonadal function, and skeletal development. J. Pediatr. *144*, 274–277.
15. Pachlopnik Schmid, J., Lemoine, R., Nehme, N., Cormier-Daire, V., Revy, P., Debeurme, F., Debré, M., Nitschke, P., Bole-Feysot, C., Legeai-Mallet, L., et al. (2012). Polymerase ε1 mutation in a human syndrome with facial dysmorphism, immunodeficiency, livedo, and short stature ("FILS syndrome"). J. Exp. Med. *209*, 2323–2330.
16. Thiffault, I., Saunders, C., Jenkins, J., Raje, N., Canty, K., Sharma, M., Grote, L., Welsh, H.I., Farrow, E., Twist, G., et al. (2015). A patient with polymerase E1 deficiency (POLE1): clinical features and overlap with DNA breakage/instability syndromes. BMC Med. Genet. *16*, 31.
17. Bellelli, R., Borel, V., Logan, C., Svendsen, J., Cox, D.E., Nye, E., Metcalfe, K., O'Connell, S.M., Stamp, G., Flynn, H.R., et al. (2018). Polε Instability Drives Replication Stress, Abnormal Development, and Tumorigenesis. Mol. Cell *70*, 707–721.e7.
18. Arboleda, V.A., Lee, H., Parnaik, R., Fleming, A., Banerjee, A., Ferraz-de-Souza, B., Délot, E.C., Rodriguez-Fernandez, I.A., Braslavsky, D., Bergadá, I., et al. (2012). Mutations in the PCNA-binding domain of CDKN1C cause IMAGe syndrome. Nat. Genet. *44*, 788–792.
19. Hamajima, N., Johmura, Y., Suzuki, S., Nakanishi, M., and Saitoh, S. (2013). Increased protein stability of CDKN1C causes a gain-of-function phenotype in patients with IMAGe syndrome. PLoS ONE *8*, e75137.
20. Shcherbakova, P.V., Pavlov, Y.I., Chilkova, O., Rogozin, I.B., Johansson, E., and Kunkel, T.A. (2003). Unique error signature of the four-subunit yeast DNA polymerase epsilon. J. Biol. Chem. *278*, 43770–43780.
21. Borges, K.S., Arboleda, V.A., and Vilain, E. (2015). Mutations in the PCNA-binding site of CDKN1C inhibit cell proliferation by impairing the entry into S phase. Cell Div. *10*, 2.
22. Gaillard, H., García-Muse, T., and Aguilera, A. (2015). Replication stress and cancer. Nat. Rev. Cancer *15*, 276–289.
23. Furstenthal, L., Swanson, C., Kaiser, B.K., Eldridge, A.G., and Jackson, P.K. (2001). Triggering ubiquitination of a CDK inhibitor at origins of DNA replication. Nat. Cell Biol. *3*, 715–722.
24. Chuang, L.C., and Yew, P.R. (2005). Proliferating cell nuclear antigen recruits cyclin-dependent kinase inhibitor Xic1 to DNA and couples its proteolysis to DNA polymerase switching. J. Biol. Chem. *280*, 35299–35309.
25. Hughes, C.R., Guasti, L., Meimaridou, E., Chuang, C.H., Schimenti, J.C., King, P.J., Costigan, C., Clark, A.J., and Metherell, L.A. (2012). MCM4 mutation causes adrenal failure, short stature, and natural killer cell deficiency in humans. J. Clin. Invest. *122*, 814–820.
26. Frugoni, F., Dobbs, K., Felgentreff, K., Aldhekri, H., Al Saud, B.K., Arnaout, R., Ali, A.A., Abhyankar, A., Alroqi, F., Giliani, S., et al. (2016). A novel mutation in the POLE2 gene causing combined immunodeficiency. J. Allergy Clin. Immunol. *137*, 635–638.e1.
27. Guernsey, D.L., Matsuoka, M., Jiang, H., Evans, S., Macgillivray, C., Nightingale, M., Perry, S., Ferguson, M., LeBlanc, M., Paquette, J., et al. (2011). Mutations in origin recognition complex gene ORC4 cause Meier-Gorlin syndrome. Nat. Genet. *43*, 360–364.
28. Burrage, L.C., Charng, W.L., Eldomery, M.K., Willer, J.R., Davis, E.E., Lugtenberg, D., Zhu, W., Leduc, M.S., Akdemir, Z.C., Azamian, M., et al. (2015). De Novo GMNN Mutations Cause Autosomal-Dominant Primordial Dwarfism Associated with Meier-Gorlin Syndrome. Am. J. Hum. Genet. *97*, 904–913.

The American Journal of Human Genetics, Volume *103*

Supplemental Data

DNA Polymerase Epsilon Deficiency Causes

IMAGe Syndrome with Variable Immunodeficiency

Clare V. Logan, Jennie E. Murray, David A. Parry, Andrea Robertson, Roberto Bellelli, Žygimantė Tarnauskaitė, Rachel Challis, Louise Cleal, Valerie Borel, Adeline Fluteau, Javier Santoyo-Lopez, SGP Consortium, Tim Aitman, Inês Barroso, Donald Basel, Louise S. Bicknell, Himanshu Goel, Hao Hu, Chad Huff, Michele Hutchison, Caroline Joyce, Rachel Knox, Amy E. Lacroix, Sylvie Langlois, Shawn McCandless, Julie McCarrier, Kay A. Metcalfe, Rose Morrissey, Nuala Murphy, Irène Netchine, Susan M. O'Connell, Ann Haskins Olney, Nandina Paria, Jill A. Rosenfeld, Mark Sherlock, Erin Syverson, Perrin C. White, Carol Wise, Yao Yu, Margaret Zacharin, Indraneel Banerjee, Martin Reijns, Michael B. Bober, Robert K. Semple, Simon J. Boulton, Jonathan J. Rios, and Andrew P. Jackson

Supplemental Note: Case Reports

Skeletal Features: Metaphyseal dysplasia was a defining feature of the original IMAGe association[1]. In these initial case reports, the metaphyses were reported to be striated and irregular. Osteopenia, delayed bone age and small epiphyses were also noted. With the identification of *CDKN1C* mutations as a cause of IMAGe syndrome, it became evident that metaphyseal changes and the other skeletal findings were variably present and could be expanded to include scoliosis[2]. The identified skeletal abnormalities are age-dependent, can be absent or subtle[3] and most commonly manifest as delayed bone age and short stature[3]. Similar skeletal involvement is seen in *POLE* deficient IMAGe subjects, with generalised undermineralisation (osteopenia) and bilateral hip dysplasia being the most commonly reported (n=8). Metaphyseal widening and striations were previously reported in P13[4] and P12[5]. P1 and P6 also have metaphyseal involvement characterized by a sclerotic metaphyseal band and mild widening. Scoliosis (n=3), increased epiphyseal density in distal phalanges (n=1), 11 rib pairs (n=2), absent/hypoplastic patella (n=2), brachydactyly (n=1) were reported in other cases. P4 had no clear metaphyseal abnormalities (though growth plates were closed in this adult patient, age 50), however osteopenia and an increased upper thoracic kyphosis were present. Metaphyseal striations were also reported with the previously reported c.4444+3A>G mutation (which was denoted, 'FILS syndrome', mild facial dysmorphism, immunodeficiency, livedo, and short stature)[6].

Habitus: In the three adult subjects (P1, 4, 10), central adiposity and thin extremities were noted.

Neurocognition: Developmental delay/learning disability varied from normal or mild speech delay to moderate-severe impairment. Three individuals developed seizures with at least two occurring in childhood. MRI neuroimaging, normal (n=3), pituitary hypoplasia (P7, P13, P15), hypoplastic corpus callosum with small flattened pituitary and ventriculomegaly (P5); prominent extra-axial CSF with some periventricular high signal in frontal lobes (P1).

Infancy: Many families reported feeding difficulties as neonates, with six subjects progressing to gastrostomy insertion. Early respiratory problems were also noted included tracheomalacia and respiratory distress requiring CPAP support. Hypoglycaemia was also reported.

Malformations: Malformations were uncommon: atrial septal defect (P7), and unilateral hydronephrosis with proximal hydroureter (P3).

Supplemental Figures

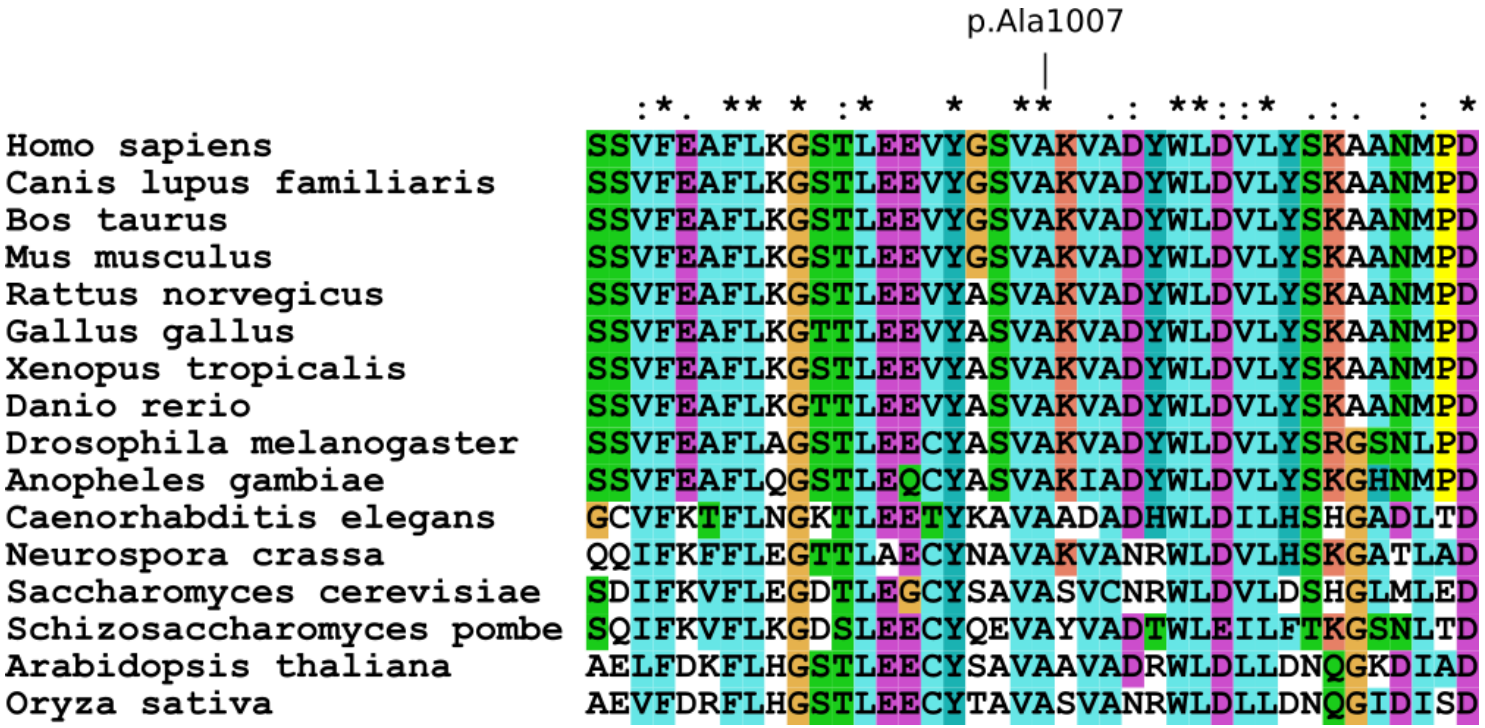

Figure S1: ClustalX alignment of POLE1 orthologs showing human p.Ala1007 and flanking residues.
The position of human alanine 1007 (mutated to proline in patient P10) is marked above the alignment. Asterisks indicate fully conserved positions, colons indicate positions with conservation between groups of strongly similar properties (PAM250 score > 0.5) and dots indicate conservation between groups with weakly similar properties (PAM250 score ≤ 0.5). Protein accessions used: Homo sapiens, NP_006222.2; Canis lupus familiaris, XP_543348.3; Bos taurus, NP_001178358.1; Mus musculus, NP_035262.2; Rattus norvegicus, NP_001100622.2; Gallus gallus, XP_004934482.1 ; Xenopus tropicalis, XP_004910692.1; Danio rerio, NP_001121995.1; Drosophila melanogaster, NP_524462.2; Anopheles gambiae, XP_315205.4; Caenorhabditis elegans, NP_493616.1; Neurospora crassa, XP_955939.2; Saccharomyces cerevisiae, NP_014137.1; Schizosaccharomyces pombe, NP_596354.1; Arabidopsis thaliana, NP_172303.5; Oryza sativa, NP_001046939.2.

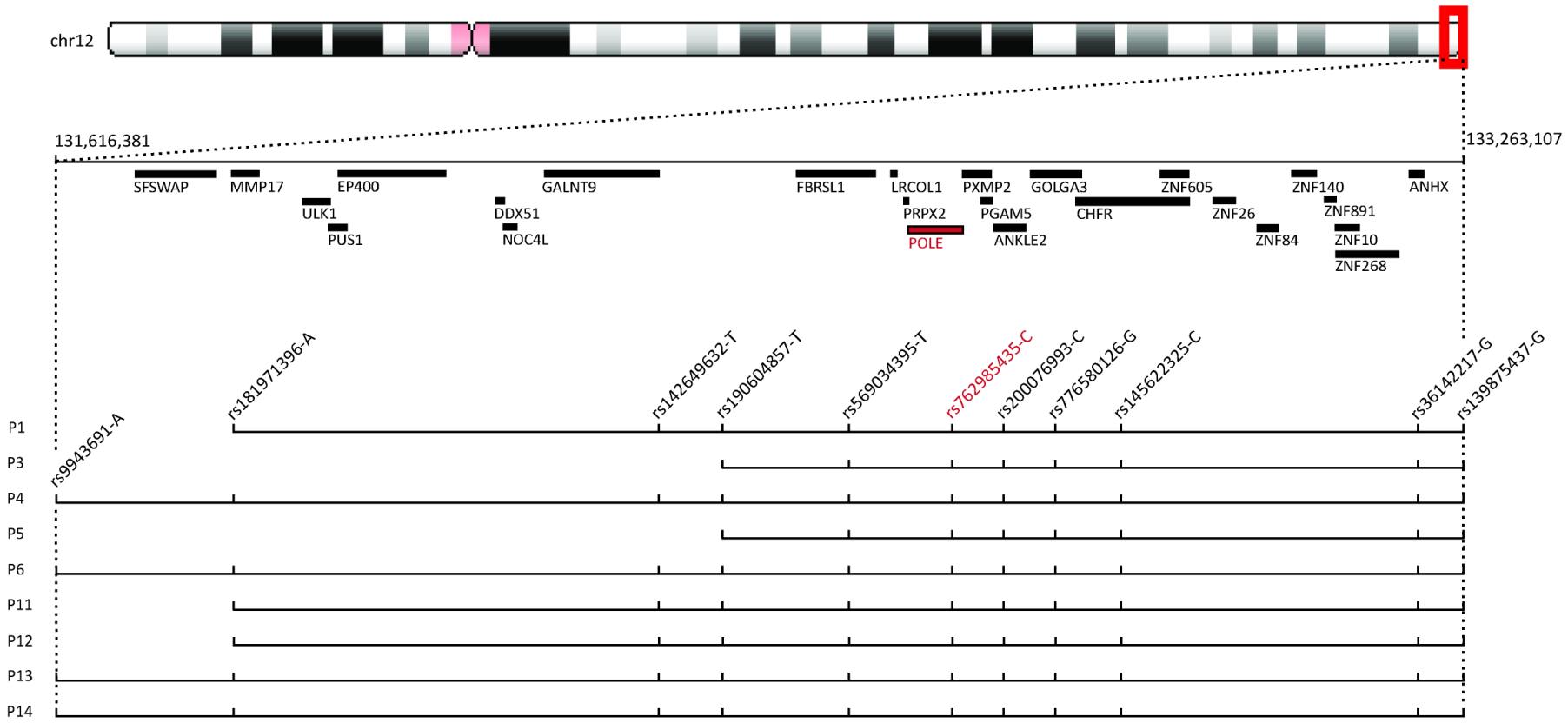

Figure S2: Schematic of region of chromosome 12q24.33, depicting shared haplotype region.
rs762985435 (red), c.1686+32C>G *POLE.* dbSNP identifiers and the allele present on the shared haplotype provided. Lines indicate the extent of the shared haplotype for different subjects.

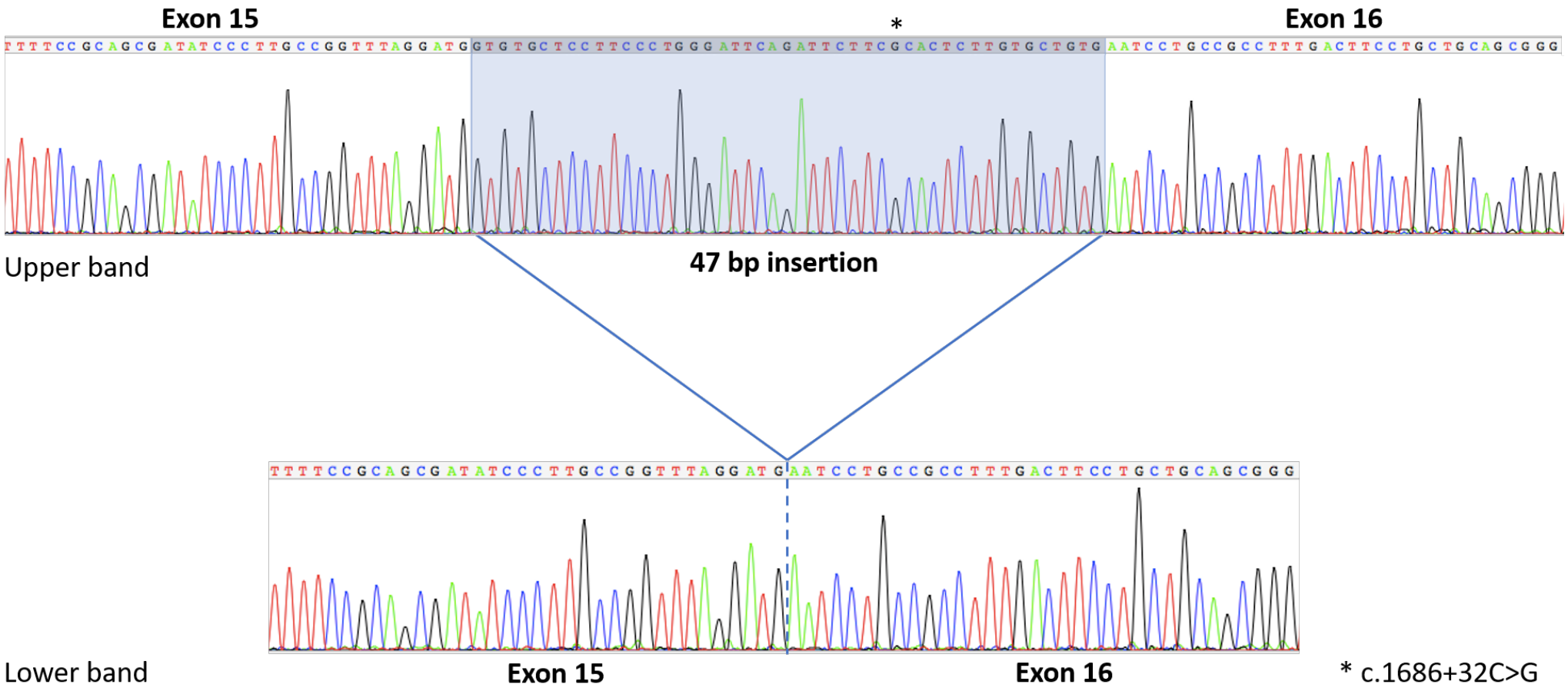

Figure S3: Representative Sanger sequencing electropherograms of POLE transcripts from P1.
POLE cDNA amplified with primers as indicated in Fig 3A, with sequence corresponding to upper and lower bands in this figure panel. The upper band includes 47 bp of intron 15 (highlighted in blue). The c.1686+32C>G variant is evident in the retained intronic sequence, indicated by asterix.

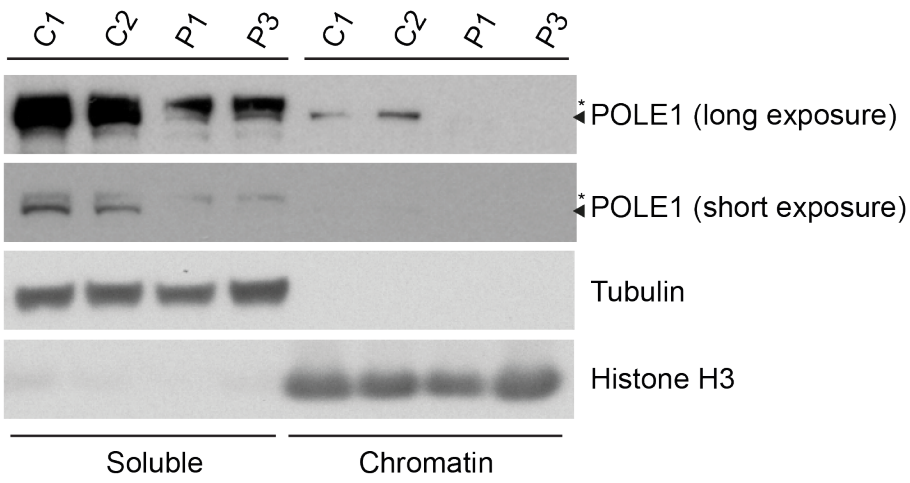

Figure S4. Chromatin Fractionation and Immunoblotting of POLE1
Western blot analysis of POLE1 from total soluble and chromatin fractions of control (C1, C2) and patient derived (P1, P3) primary fibroblasts lines. Antibody (GTX132100) raised against recombinant protein encompassing a sequence within the N-terminus region of human POLE1. Tubulin and Histone H3, loading controls respectively for soluble and chromatin-associated proteins. * denotes, non-specific band. Short exposure, ~30s; long exposure, ~20mins.

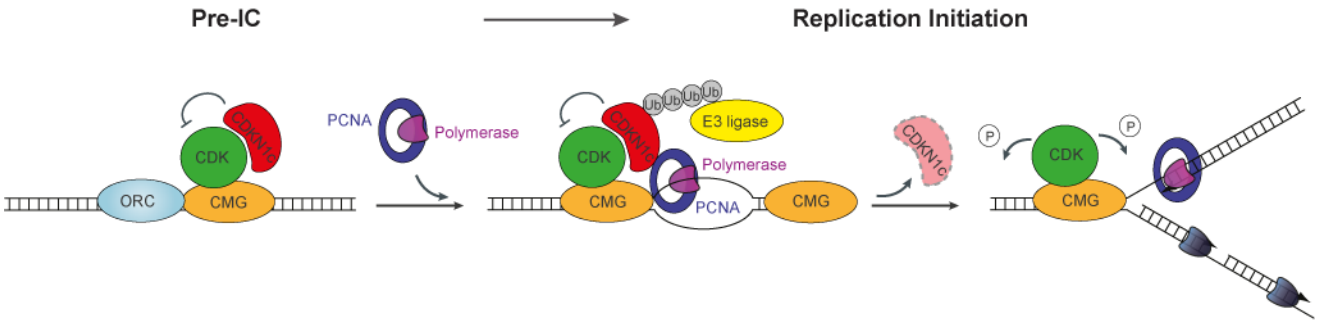

Figure S5. Hypothetical model of functional relationship between CDKN1C and PCNA/DNA polymerase loading.

Mutations in POLE1 and CDKN1C both cause IMAGe syndrome, suggesting a potential functional relationship. PCNA is required for CDKN1C ubiquitination[2], and overexpression experiments have established that CDKN1C-IMAGe mutations both disrupt PCNA binding[2] and result in increased protein stability[7; 8]. However the context, cell-cycle timing and location for PCNA binding and CDKN1C degradation has not yet been established. Biochemical studies on Xenopus CDKN homologs using egg extracts suggest that CDKNs may inhibit CDK activity, until PCNA/polymerase loading onto DNA triggers their ubiquitination and proteolytic degradation during replication fork initiation[9; 10]. The relevance of these findings to somatic mammalian cells and CDKN1C remain to be determined. CDK, Cyclin dependent kinase; ORC, Origin Recognition Complex; CMG complex (CDC45, MCM2-7, GINS); Ub, ubiquitin; P, phosphorylation of target proteins by CDK.

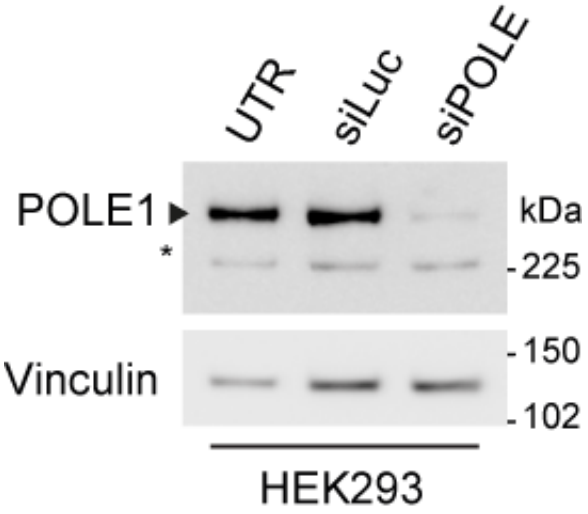

Figure S6. **Validation of POLE1 monoclonal antibody (93H3A)**.
The antibody used (93H3A) was raised against recombinant human POLE1 corresponding to aa1-176. UTR, untransfected. siLuc, negative siRNA control. siPOLE, siRNA targeting *POLE* transcript. *, non-specific band. Vinculin was used as a loading control.

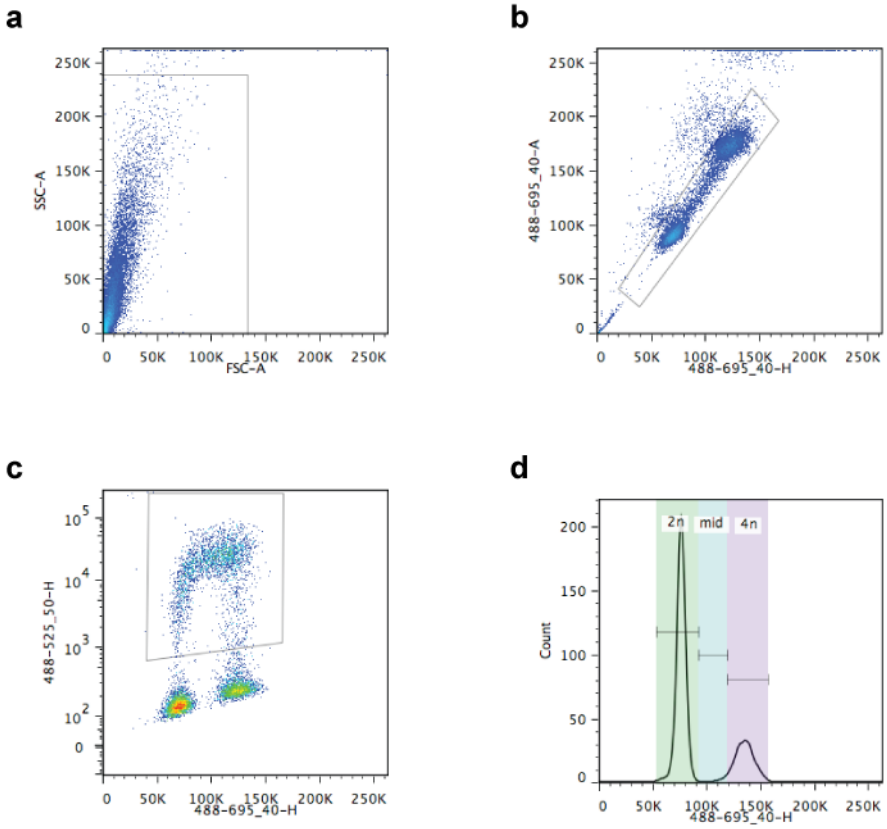

Figure S7. Gating strategy for FACS-cell cycle analysis, for experiment depicted in Fig 3c,d. Cells gated on FSC/SSC as indicated (**a**), and doublet cells then removed (**b**). BrdU-labelled population then gated (**c**), and 2n, 4n and mid-S phase populations defined (**d**). Representative plots for C1, 0 h time point (a-c), except bottom right (d) C1, 8 h time point shown, as 2n, 4n populations are most distinct at this time point

Supplemental Tables

	Primordial dwarfism	**gnomAD All Populations**
LoF	3	198
No LoF	93	277078
***P*-Value**	5.10×10^{-5}	

Table S1. *POLE* Allele counts. Whole-genome sequenced subjects from Primordial dwarfism cohort (n=48) versus gnomAD database (n=138,638, WGS/WES). *P*-value, one-tailed Fisher's exact test. LoF, loss of function.

ID	Prenatal Growth				Postnatal growth			
	Gest^{n} /wks	Weight /kg (s.d.)	Length /cm (s.d.)	OFC /cm (s.d.)	Age at exam	Weight /kg (s.d.)	Height /cm (s.d.)	OFC /cm (s.d.)
P1	31	0.926 (-2.8)	35* (-5.8)	26.6 (-2.0)	18yrs	18.25 (-14)	109.9 (-9.6)	48.5 (-5.1)
P3	41	2.5 (-2.6)	n/a	34.8 (-0.8)	7yrs	15 (-3.9)	93.8 (-5.5)	49.4 (-2.7)
P4	40+6	2.49 (-2.4)	n/a	n/a	50yrs	n/a	88 (-12.5)	46 (-8.03)
P5	39	2.4 (-2.1)	42.5 (-3.9)	34 (-0.5)	11yrs 7mths	14.3 (-8.6)	99.2 (-6.8)	47.4 (-4.7)
P6	35	1.42 (-2.8)	40 (-3.5)	28 (-2.8)	9yrs 6mths	15 (-5.3)	100.7 (-5.7)	46.7 (-5.5)
P7	38	2.1 (-2.4)	41.9 (-3.8)	n/a	13yrs	20.1 (-5.3)	106.1 (-6.2)	47 (-5.2)
P8	34	1.3 (-2.8)	n/a	n/a	2yrs 9mths	5 (-10.4)	66.6 (-7.5)	41 (-7.3)
P9	37	1.56 (-3.3)	n/a	n/a	1yr 7mths	4.4 (-9.3)	59.2 (-7.7)	42.5 (-4.7)
P10	40	1.45 (-4.9)	42 (-4.4)	32 (-2.1)	39yrs	13.8 (-16.8)	95.6 (-11.27)	n/a
P11	37	1.4 (-3.8)	39 (-4.8)	29 (-3.0)	-	n/a	n/a	n/a
P12	34	1.26 (-2.8)	38 (-4.2)	28 (-2.3)	12yrs	11 (-9.14)	113 (-5.07)	At 6 months 35.5 (-5.8)
P13	40	2.07 (-3.2)	42 (-4.5)	33 (-1.7)	-	n/a	n/a	n/a
P14	36	1.8 (-2.2)	44 (-1.7)	32.5 (-0.2)	18yrs 7mths	24.5 (-7.9)	112.7 (-8.4)	n/a
P15	40	1.35 (-3.9)	40 (-4.3)	30.5 (-2.2)	31yrs	16.8 (-15.6)	103 (-10.6)	'microcephaly'

Table S2: Anthropometric measurements in *POLE* individuals with biallelic mutations. ID, Individual number. Gest^{n}, gestation. wks, weeks. s.d., Z-scores calculated with LMS growth using British 1990 dataset. *measurement at age 3 weeks (first available postnatal measurement). P15 OFC measurement not available but documented to have microcephaly although OFC not as severe as height.

ID	Age	Endocrine			Genitourinary		Skin			
		Adrenal Insufficiency	Age at diagnosis	Additional Information	Hypospadias	Bilateral Cryptorchidism	Eczema	Café aux lait	Livedo	Additional Information
P1	18yrs	Y	18mths	Presented in adrenal crisis. Developed Insulin resistance, delayed puberty, fatty liver & hypertriglyceridaemia (likely related to stem cell transplant)	Y	Y (descended later in childhood)	Y	N	N	
P3	7yrs	Y	5yrs	Presented with hypoglycaemic episodes. No response to GH therapy	Y (mild)	Y (hypoplastic scrotum)	N	N	N	
P4	50yrs	N	-	Normal cortisol but dynamic testing not performed	Female	Female	Y	N	N	
P5	11yrs 7m	Y	7yrs	Neonatal hypothyroidism. Panhypopituitarism at 12 months including GH deficiency. Small, flattened pituitary on MRI.	Y	Y	N	N	N	
P6	9yrs 6m	Y	Neonate	Nephrocalcinosis & hypercalciuria at 6mths. GH deficiency.	Female	Female	N	N	Intermittent	Psoriasis from 11 yrs, Livedo improved with age
P7	13yrs	Y	Neonate	Low GH identified at 14mths, low ACTH at 22mths with low cortisol, hypothyroid at 3yrs	Y (ambiguous genitalia)	Y	Y	N	N	
P8	4yrs 2m	Y	4yrs	Hyponatraemia identified during prolonged viral infection. GH deficiency.	N	Y	N	N	N	
P9	2yrs 3m	N	-	Normal cortisol but dynamic testing not performed	Female	Female	N	N	N	
P10	39yrs	Y	Neonate	Pigmentation at birth. Presented with salt wasting crisis. GH deficiency but no response to GH therapy.	Female	Female	N	Y	N	
P11	3m	N	-	-	Female	Female	N	Y	N	
P12	12yrs	Y	Neonate	No response to GH therapy. Diabetes. Affected sister (P11) found to have small adrenal glands with abnormal cortex and small pituitary on post-mortem examination	Female	Female	N	N	N	

P13	8yrs	Y	4yrs 6mths	Progressive pigmentation at 4yrs. Small anterior pituitary on MRI. GH deficiency but no response to GH therapy.	Y	Y	N	Y	N	
P14	18yrs 7m	Y	4yrs	Hyponatraemic seizure at 4yrs. Hypercalcaemia in infancy. Normal cortisol at 6mths. Severe failure to thrive, chronic diarrhoea and pancreatic enzyme deficiency. GH deficiency with no response to GH therapy	Female	Female	N	Y	N	
P15	31yrs	Y	2yrs	Presented with hypoglycaemia & seizures at 2yrs. Pituitary hypoplasia on MRI.	N	Y	N	Y	N	

Table S3: Endocrine, Genitourinary, Immune and Skin findings in POLE deficient individuals. ID, Individual number. Growth Hormone (GH) deficiency established through provocative testing. P1, developed lactic acidosis during trial of metformin. Yrs, years; m, months.

ID	Clinically increased infection Y/N	Bacterial	Viral	Fungal	Neutro-phils X 10^9/L *(normal range)*	Lymphocyte Subsets				Immunoglobulins			Additional Information
						CD3+CD4+ X 10^6/L	**CD3+CD8+** X 10^6/L	**CD19** X 10^6/L	**NK cells** X 10^6/L	**IgG** g/L	**IgA** g/L	**IgM** g/L	
P1	Y	Pseudomonas aeruginosa, Klebsiella pneumoniae	CMV Severe EBV (required BMT)	Candida albicans	Normal 3-4.8 (1.5-8)	Normal 1040 (300-2000)	Normal 770 (300-1800)	Low <10 (200-1600)	Low 10 (90-900)	Normal 10.4 (7.68-17.28)	Normal-High 6.41 (0.77-1.67)	Low 0.28 (0.57-2.66)	EBV haemophagocytic lymphohistiocytosis requiring stem cell transplant. Severe local reactions to immunisations. Normal response to tetanus, moderate response to HiB, absent response to pneumococcus
P2	Y	N	HSV	N	n/a	n/a	n/a	n/a	n/a	n/a	n/a	n/a	Died at 22 mths secondary to HSV infection
P3	Y	N	N	N	Normal 5.26 (1.5-8)	Normal 46% (31-47)	Normal 36% (18-35)	Low-normal 239 (270-860)	Low 50 (100-480)	Normal 9.3 (5.4-16.1)	High-Normal 2.82 (0.7-2.5)	Low-Normal 0.46 (0.5-1.8)	Recurrent otitis media
P4	Y	Y	N	N	n/a	Normal 990 (600-1700)	Low 30 (400-1000)	Normal 170 (40-500)	Normal	n/a	n/a	n/a	IgM paraproteinaemia Affected sister died of respiratory infection
P5	Y	Y	Y	N	n/a	n/a	n/a	n/a	n/a	n/a	n/a	n/a	Poor response to vaccines. Recurrent pneumonia, urinary tract and upper respiratory tract infections. Chronic lung disease and bronchiectasis. Peripheral T cell lymphoma at 11yrs (large cell type)
P6	Y	Y Grp A strep	Y Influenza	N	Normal 5.38	n/a	n/a	n/a	n/a	n/a	n/a	n/a	

			RSV		(1.5-7.4)								
P7	N	N	N	N	n/a	n/a	n/a	n/a	n/a	n/a	n/a	n/a	
P8	Y	Y	Y Astrovirus EBV	N	Normal 5.64 (1.5-8.5)	Normal 1236 (850-1800)	Low 390 (650-1500)	Low-normal 552 (600-1300)	Low 98 (180-600)	Normal 6.73 (4-16)	Normal 2.97 (0.4-2)	Normal 0.64 (0.5-2)	Normal response to vaccine*
P9	Y	Y	Y Norovirus	N	Normal	Normal 1853 (850-1800)	Low 451 (650-1500)	Normal 1079 (600-1300)	High 1018 (180-600)	Normal 3.5 (3.1-13)	Normal 0.71 (0.3-1.2)	Low 0.31 (0.5-2.2)	Normal response to vaccine*
P10	N	N	N	N	Normal 2.8 (1.5-8)	Normal	Normal	Normal	Normal	1.8	4.3	1.7	
P11	Y	Klebseilla	N	N	n/a	n/a	n/a	n/a	n/a	n/a	n/a	n/a	Died at 3months with Klebsiella pneumonia.
P12	N	N	N	N	n/a	n/a	n/a	n/a	n/a	n/a	n/a	n/a	
P13	N	N	N	N	n/a	n/a	n/a	n/a	n/a	n/a	n/a	n/a	
P14	Y	Y MRSA	N	Y Candida	Normal 1.53 (1.0-8.53)	Low 753 (2815-6110)	Low 252 (394-1637)	Normal 991 (179-2657)	n/a	Low 1.5 (2.86-16.80)	Normal 0.11 (0.1-1.29)	Normal 0.25 (0.21-1.92)	Chronic cutaneous candidiasis & MRSA infection, T cell proliferative responses normal
P15	Y	N	Y	N	n/a	n/a	n/a	n/a	n/a	Normal	Low	Undetec-table	Chronic otitis media, nodular sclerosis Hodgkin's lymphoma at 28yrs

Table S4: Immunological Phenotype in POLE deficient individuals. Values included where available. Normal reference range for diagnostic lab where test performed in brackets. *Measured for Hib, Tetanus and Pneumococcus. n/a not available. BMT Bone Marrow Transplant.

Syndrome	Clinical Features	Gene(s)	Inheritance	Molecular mechanism	References
FILS	Facial Dysmorphism, Immunodeficiency, Livedo and Short Stature	*POLE* (2 families)	AR	Biallelic partial loss of function, homozygous splice mutation predicted to reduce levels of Polymerase Epsilon	Schmid *et al*, 2012[6], Thiffault *et al,* 2015[11]
IMAGe Syndrome	Intrauterine Growth Restriction, Metaphyseal dysplasia, Adrenal Insufficiency, Genitourinary abnormalties in males Plus variable immunodeficiency (POLE only)	*CDKN1C* *POLE*	AD (maternal allele only) AR	Imprinted gain of function mutations in PCNA binding domain. Biallelic loss of function mutations predicted to reduce levels of Polymerase Epsilon.	Arboleda *et al,* 2012[2] Current manuscript
MCM4 deficiency	Severe pre- and post-natal growth failure, Microcephaly, Immunodeficiency (decreased NK cells), Adrenal Insufficiency and cancer predisposition	*MCM4*	AR	Biallelic partial loss of function, homozygous splice mutations	Casey *et al*, 2012[12], Eidenschenk *et al*, 2006[13], Gineau *et al*, 2012[14], Hughes *et al*, 2012[15].
GINS1 deficiency	Intrauterine growth deficiency, Immunodeficiency (NK cell deficiency and chronic neutropenia), eczema	*GINS1*	AR	Biallelic partial loss of function mutations	Bernard *et al,* 2004[16], Cottineau *et al,* 2017[17]
Meier Gorlin	Microtia, Hypoplastic/Absent Patella, Short Stature Plus craniosynostosis (*CDC45* only)	*ORC1, ORC4, ORC6, CDT1, CDC6, CDC45* *GMNN*	AR AD	Biallelic partial loss of function mutations, impaired replication licencing *De novo* gain of function mutations	Bicknell *et al,* 2011[18; 19], Bongers *et al,* 2001[20], de Munnik *et al,* 2012[21], Fenwick *et al,* 2016[22] Burrage *et al,* 2015[23]
Rothmund-Thomson	Skin atrophy, telangiectasia, hyper-/hypo-pigmentation (poikiloderma congenitale), skeletal abnormalities, short stature, premature aging, cancer predisposition	*RECQL4*	AR	Biallelic loss and partial loss of function mutations	Kitao *et al,* 1999[24], Lindor *et al,* 2000[25], Wang *et al,* 2001[26]
Baller-Gerold	Craniosynostosis, radial aplasia, growth retardation, poikiloderma				Van Maldergem *et al*, 2006[27]
RAPADILINO	Radial and patella hypoplasia/aplasia, small stature, diarhhoea in infancy, dysmorphic features, cleft/high arched palate				Kaariainen *et al,* 1989[28], Siitonen *et al,* 2003[29]

Table S5: Summary of clinical and molecular genetic findings associated with disorders of the replisome. AR Autosomal Recessive, AD Autosomal Dominant.

Materials and Methods:

Research subjects

Genomic DNA was extracted from blood samples by standard methods or from saliva samples using Oragene collection kits according to the manufacturer's instructions. Informed consent was obtained from all participating families. The studies were approved by the ethics review boards, the Scottish Multicentre Research Ethics Committee (05/MRE00/74) and the University of Texas Southwestern Medical Center. Parents provided written consent for the publication of photographs of the affected individuals.

Whole-Genome Sequencing, Whole-Exome Sequencing and Analysis

Whole Genome Sequencing in P1, P3 and P4 was performed by Edinburgh Genomics (Clinical Division) as part of the Scottish Genomes Project (SGP) to 30X coverage using TruSeq Nano library preparation kits and a HiSeq X sequencing platform (Illumina). FASTQs generated by Edinburgh Genomics were aligned to the human genome (hg38, including alt, decoy and HLA sequences) using bwa mem[30] (0.7.13). Post-processing was performed with samblaster[31] (0.1.22) to mark duplicate reads, and the Genome Analysis ToolKit[32] (GATK, v3.4-0-g7e26428) for indel realignment and base recalibration. Genotype likelihoods for each sample were calculated using the GATK HaplotypeCaller and resulting GVCF files were called jointly using GATK's GenotypeGVCFs function. Variant quality score recalibration (VQSR) was performed as per GATK best-practices[33] and a truth sensitivity threshold of 99.9% applied.

Functional annotations were added using Ensembl's Variant Effect Predictor[34] (v84). VASE (v0.1, https://github.com/gantzgraf/vase) was used to perform variant filtering and burden analysis. Variants were filtered to remove those outside the 99.9% truth sensitivity threshold from VQSR, with a frequency greater than 0.1% in gnomAD or dbSNP147, or in segmentally duplicated regions or regions of low sequence complexity. Allele counts were generated for genotype calls with a minimum PHRED scale genotype quality score of 20 for each canonical transcript in the GENCODE basic transcript set where the alternative allele resulted in predicted loss of function (stop gain, stop loss, splice donor/acceptor site disruption or indels resulting in frameshifts). Allele counts per transcript were compared with variant data from gnomAD[35].

WGS in P10-14 was performed by the Hudson Alpha Genome sequencing Centre to an average 40X coverage using a HiSeq platform (Illumina) and analysed using DRAGEN software (Edico Genome). Whole Exome Sequencing in P5 and P6 was performed as described previously[36]. WES in P15 was performed as previously described[37; 38].

All *POLE* variants identified were confirmed by capillary sequencing, using standard methodology. Details of primers listed below.

Haplotype Analysis

Variants surrounding rs762985435 were identified from WGS and WES VCF files and analysed for shared haplotypes in samples with this SNP using bespoke software (available at https://github.com/gantzgraf/het_hap_phaser).

Cell Culture

Primary dermal fibroblasts (Patient P2, P3) were established from skin punch biopsies in AmnioMax medium (Life Technologies) and then maintained in Dulbecco's MEM (modified Eagle's medium; DMEM) supplemented with 10% fetal bovine serum, 5% L-glutamine and 5% penicillin/streptomycin, at 5% CO_2 and 3% O_2. Patient 1 primary fibroblasts were a kind gift from Prof. Penny Jeggo, University of Sussex. Genotypes of patient cell lines were validated by Sanger sequencing and immunoblotting.

RT-PCR

Total RNA was extracted from cell lines using the RNeasy kit (Qiagen) according to the manufacturer's instructions. Following DNase I (Qiagen) treatment cDNA was generated using SuperScript III Reverse Transcriptase kit (Thermo Fisher Scientific). RT-PCR was performed on cDNA using primers in exon 14 and 17 (details below).

Mini-Gene Assay

A 1.6 kb stretch of the *POLE* gene encompassing the 3' end of intron 12, exon 13, intron 13, exon 14, intron 14, exon 15, intron 15, exon 16 and the 5' end of intron 16 was amplified using DNA from control genomic DNA with SalI-pole-int12-F and XbaI-pole-int16-R primers, and cloned into the RHCglo vector[39] using SalI and XbaI restriction sites. Site-directed mutagenesis was used to introduce the *POLE* intron 15 patient mutation c.1686+32C>G and as a positive control, *POLE* intron 15 splice donor mutation (c.1686+1G>A) into the splicing reporter construct. HeLa cells were transfected with each individual splicing mutation reporter construct using Lipofectamine 2000 according the manufacturer's instructions. Twenty-four hours after transfection, cells were harvested, total cellular RNA extracted, and cDNA generated using Superscript III reverse transcriptase first-stand synthesis system (Invitrogen). PCR was carried out using primers (RSV5U-minigene-F and RTRHC-minigene-R) to the 5' and 3' ends of the artificial exons present in the RHCglo vector. cDNA amplicons for WT and mutated *POLE* were resolved on a 2% agarose gel to visualize differences in splicing. Individual PCR products were subsequently cloned into the pGEM-T Easy Vector (Promega) and sequenced to verify the exon content of each transcript. All relevant primers details are listed below.

Western blot analysis and antibodies

Whole cell extracts were obtained by lysis and sonication of cells in UTB buffer (8 M Urea, 50 mM Tris pH 7.5, 150 mM β-mercaptoethanol, protease inhibitor cocktail (Roche)) or in NP-40 lysis buffer 23(50 mM Tris pH 8.0, 280 mM NaCl, 0.5% NP-40, 0.2 mM EDTA, 0.2 mM EGTA, 10% Glycerol, 1 mM DTT, protease inhibitor cocktail (Roche), 1 mM PMSF, phosphatase inhibitors (40 mM NaF, 1 mM sodium orthovanadate)) and analyzed by SDS-PAGE following standard procedures. Protein samples were run on 6-12% acrylamide SDS-PAGE or 4-12% NuPage mini-gels (Life Technologies) and transferred onto nitrocellulose membrane. Immunoblotting was performed using antibodies to POLE (93H3A clone; Thermofisher Scientific cat# MA5-13616 at 2 µg/ml) and Vinculin (2C6-1B5 clone; Novusbio cat# H00007414-M01 1/5,000 dilution) (Figure S6). Chromatin fractionation experiments were performed as described in Bellelli *et al*., 2014[40], immunoblotting with POLE antibody, GTX132100, GeneTex.

FACS analysis

Non-confluent, primary fibroblasts grown in AmnioMax medium (Life Technologies) were pulse labeled with 10 µM BrdU for 30 min, washed and then harvested at 0, 4 and 8 h time points before fixation with 70% ethanol at -20°C for 16 h. Fixed cells were then digested with 1 mg/ml pepsin, denatured in 2 M HCl, and washed with PBS. After blocking in 0.5% BSA, 0.5% Tween-20, BrdU labelling was detected using anti-BrdU antibody (Abcam, ab6326; 1:75) and FITC-conjugated anti-rat secondary antibody, and DNA content determined by co-staining with 50 µg/ml propidium iodide. Cells were sorted on a BD Biosciences FACS Aria II and data analyzed using FlowJo software (v7.6.1, Tree Star) (Figure S7).

Code Availability

All custom code used in this study available at github.com (https://github.com/gantzgraf/vase and https://github.com/gantzgraf/het_hap_phaser) licensed under the MIT free software license.

Primer sequences for screening of *POLE* exons and flanking sequences

Exon	Forward Primer Sequence 5'-3'	Reverse Primer Sequence 5'-3'
1	ATTTCCGGCTCTCGCGAG	CCCTACCCCAGTCAGGCG
2	TGTCGCCTGTGGTCCCAG	CTCATGTGTCCCCCACTCTT
3	AGTGCTGAGTTTCCCGAAAG	CCTCCCTGACAGTCACAGAG
4	GGAGCAAGCAATGTGTTTTCA	GCTCACAACCCTAATCAGGATC
5	CTGTGGTGGGCTTTGCAAC	GATCCCACCTGCCAGGAA
6	GTGCAGAGTTGGACAAGGTG	ACAGAGCCAGCCATTAAGGT
7	TCCTCGGTTTGAACTCTGGT	CCTGCAAAACACACAGTGTG
8	GCCTCTCCATTGACCTGAAG	TTTGGGGGAAAAGCAGCAAA
9	AGAGGGAGGTAGAGCAGGC	AACAGTGGGGCAGATGCT
10	TAGGCAGAGTGTGTGGGC	GCCTGAGGCCTTGGAAAGAT
11	ACTTTGGGAGAGGAATTTGGAA	CTAAGTCGACATGGGAAGCG
12	GGGAGGAATGGAGAAAGGGG	GATGTGGTGACAGCACAGTC
13	GTTTTGCCAGTTCTCAGGGG	AGGACAAAACACGTGTGTCC
14	CAGGCTTTGCTTTCTGTGCT	CAGCTCCAGTGCATTTGGAA
15	TAGGTTCCTGGACTTTGCCT	TGGGACAGGATGGGGAGA
16	GAGCTTTCTCGGGCACAAC	CTGCTGAAAGACGTGGTCTG
17	AAAAGGGGTTGGTGAACTGC	TTCGTCCACCATGGCAGAG
18	GCCTGCAGGTGAGACTTTAC	CAAAAGGAGGCACAGACACA
19	GGGCGAGTTCAGTGAGTGT	CCAGCTGGGATGGACCAA
20	ATGTTCTTCAGCACCCCTGT	AGTGCCCACTTCATGAGCC
21	TGTACACTCTTCATTGTACTGGT	TGAATCAGATGAACGGCCCT
22	CCTCCTCCCTACTCCTCACT	TTCCTTCCTGCCCAGTGTG
23	GAAGGAGGGAAGGCTGGAG	TGCAGAGCCAGTGACATCAG
24	TGTGGAAAAGCCTCGGTTTG	ATCCTGGCTCCTGATCCAAC
25	AGAGGATGAGGCACAGCTG	TGTTCTTCGGTCACCTTGGT
26	CTAGAGGAGCACAGTCCAGG	TGGACACTTATGCCATCCCC
27	CGTCCTTATTTCCATGTTCATTTGA	AGTGAAGACGCCAGACAAAA
28	CCTGTGCTCAGCATGAAGTG	AGGCCAACACCCATCAGAG
29	GCGCCATCCAGAAGATCATC	CACTACAGCACACACAGCAG
30	CAATTCTCCTGTCTTGGCCT	CTCCCTAGGGGTCAGGAC
31	GGAGGCTGCTTGTGAGAAAG	CTCCCATCCCAGACCTCAG
32	CATCGTAGGGAGGCCTAAGG	TCACACACGTTGTTTTGAGGA
33	AGGACTCCGAATAGCGTGTG	GACTTCTGCCCGGGATGT
34	ATCCCGGGCAGAAGTCAC	GCGGATACTCCCTGGAGAAG
35	AGTTCAGCTACCTGGAACCA	GGACAAGACCTGGAGGGC
36	CTTTGCCCATGAGTGCTTGT	CCTGGGTCAAGGCAAAATGG
37	GCTGTGTGAGCCCCATCTT	CACCAGGGCACAGGTCAG
38	TACTGTCGTTGTGGGCCAG	TGCCTTGAGAAGATGTCACAG
39	CTGGTTCTGGAGGTGGTGG	GCCCAATGGACCCTGTCTTA
40	GGGAAAACCTGTGCCCATTT	CATGTCTCTGGTTCTGGGGA
41	ACCCTCAGCTCTTTTCCCTC	GCTGCTCAGATTCACCATGG
42	ACAAGGGGAAATAAAGGAAAGTTG	CACACTGACGTGCTTGTCTG
43	AGGAAGGCCTCTGGTCAAAC	GATACCATGGCACAGGAGC
44	TCTGTGAGGCAATCTGACCA	ATAAGGATGCTGAGGGAGGG
45	GTGCCAGTGACCTAACTCCT	TACAGCCTCACCTTGCACA
46	GTTCTGGTCCAGACAGAGCA	ATCCATGTGAGTCAGAGGGG
47	ACCAGGCGCTTCTCACAG	CCCCTTGGAAGACACCAGG

Exon	Forward Primer Sequence 5'-3'	Reverse Primer Sequence 5'-3'
48	GGGATGAGGTCGTGCATTTT	TAGTGCTGGGCAATGTTCCG
49	CTCTCCCTCATCTGCCTCG	AGTGGTCTGGTCACTGGAAG

RT PCR primer sequences

RT PCR primers	sequence 5'-3'
RT PCR primer F	TCTGGCCACGTATTCTGTGT
RT PCR primer R	CTTCAGGGAGGCAAGCTTG

Primers used for minigene assay cloning, mutagenesis and PCR

Primer	sequence 5'-3'
SalI-pole-int12-F	TCTAGTCGACCTGCATGTTAGAATCATCCTG
XbaI-pole-int16-R	CTAGTCTAGAGTGGTCTGTGAAGAAGGCG
pole-c.1686+32C>G F	CTGGGATTCAGATTCTTCGCACTCTTGTGCTGTG
pole-c.1686+32C>G R	CACAGCACAAGAGTGCGAAGAATCTGAATCCCAG
pole-c.1686+1G>A F	CCCTTGCCGGTTTAGGATGATGTGCTTCTTCC
pole-c.1686+1G>A R	GGAAGAAGCACATCATCCTAAACCGGCAAGGG
RSV5U-minigene-F	CATTCACCACATTGGTGTGC
RTRHC-minigene-R	GGGCTTTGCAGCAACAGTAAC

Antibodies used in experimental procedures

Antibody	Antibody species	Application	Manufacturer	Catalogue Number
Anti-POLE Monoclonal Antibody (93H3A)	Mouse	WB	Thermo Fisher	MA5-13616
Anti-Vinculin Antibody (2C6-1B5)	Mouse	WB	Novus Biologicals	H00007414-M01
Monoclonal Anti-α-Tubulin Antibody	Mouse	WB	Sigma-Aldrich	T9026
Anti-Histone H3 antibody	Mouse	WB	Abcam	ab10799
Anti-POLE antibody	Rabbit	WB	GeneTex	GTX132100
Anti-BrdU antibody	Rat	FACS	Abcam	ab6326

References

1. Vilain, E., Le Merrer, M., Lecointre, C., Desangles, F., Kay, M.A., Maroteaux, P., and McCabe, E.R. (1999). IMAGe, a new clinical association of intrauterine growth retardation, metaphyseal dysplasia, adrenal hypoplasia congenita, and genital anomalies. J Clin Endocrinol Metab 84, 4335-4340.
2. Arboleda, V.A., Lee, H., Parnaik, R., Fleming, A., Banerjee, A., Ferraz-de-Souza, B., Delot, E.C., Rodriguez-Fernandez, I.A., Braslavsky, D., Bergada, I., et al. (2012). Mutations in the PCNA-binding domain of CDKN1C cause IMAGe syndrome. Nat Genet 44, 788-792.
3. Bennett, J., Schrier Vergano, S.A., and Deardorff, M.A. (1993). IMAGe Syndrome. In GeneReviews((R)), M.P. Adam, H.H. Ardinger, R.A. Pagon, S.E. Wallace, L.J.H. Bean, K. Stephens, andA. Amemiya, eds. (Seattle (WA).
4. Pedreira, C.C., Savarirayan, R., and Zacharin, M.R. (2004). IMAGe syndrome: a complex disorder affecting growth, adrenal and gonadal function, and skeletal development. J Pediatr 144, 274-277.
5. Tan, T.Y., Jameson, J.L., Campbell, P.E., Ekert, P.G., Zacharin, M., and Savarirayan, R. (2006). Two sisters with IMAGe syndrome: cytomegalic adrenal histopathology, support for autosomal recessive inheritance and literature review. Am J Med Genet A 140, 1778-1784.
6. Pachlopnik Schmid, J., Lemoine, R., Nehme, N., Cormier-Daire, V., Revy, P., Debeurme, F., Debre, M., Nitschke, P., Bole-Feysot, C., Legeai-Mallet, L., et al. (2012). Polymerase epsilon1 mutation in a human syndrome with facial dysmorphism, immunodeficiency, livedo, and short stature ("FILS syndrome"). J Exp Med 209, 2323-2330.
7. Hamajima, N., Johmura, Y., Suzuki, S., Nakanishi, M., and Saitoh, S. (2013). Increased protein stability of CDKN1C causes a gain-of-function phenotype in patients with IMAGe syndrome. PLoS One 8, e75137.
8. Borges, K.S., Arboleda, V.A., and Vilain, E. (2015). Mutations in the PCNA-binding site of CDKN1C inhibit cell proliferation by impairing the entry into S phase. Cell Div 10, 2.
9. Furstenthal, L., Swanson, C., Kaiser, B.K., Eldridge, A.G., and Jackson, P.K. (2001). Triggering ubiquitination of a CDK inhibitor at origins of DNA replication. Nat Cell Biol 3, 715-722.
10. Chuang, L.C., and Yew, P.R. (2005). Proliferating cell nuclear antigen recruits cyclin-dependent kinase inhibitor Xic1 to DNA and couples its proteolysis to DNA polymerase switching. J Biol Chem 280, 35299-35309.
11. Thiffault, I., Saunders, C., Jenkins, J., Raje, N., Canty, K., Sharma, M., Grote, L., Welsh, H.I., Farrow, E., Twist, G., et al. (2015). A patient with polymerase E1 deficiency (POLE1): clinical features and overlap with DNA breakage/instability syndromes. BMC Med Genet 16, 31.
12. Casey, J.P., Nobbs, M., McGettigan, P., Lynch, S., and Ennis, S. (2012). Recessive mutations in MCM4/PRKDC cause a novel syndrome involving a primary immunodeficiency and a disorder of DNA repair. J Med Genet 49, 242-245.
13. Eidenschenk, C., Jouanguy, E., Alcais, A., Mention, J.J., Pasquier, B., Fleckenstein, I.M., Puel, A., Gineau, L., Carel, J.C., Vivier, E., et al. (2006). Familial NK cell deficiency associated with impaired IL-2- and IL-15-dependent survival of lymphocytes. J Immunol 177, 8835-8843.
14. Gineau, L., Cognet, C., Kara, N., Lach, F.P., Dunne, J., Veturi, U., Picard, C., Trouillet, C., Eidenschenk, C., Aoufouchi, S., et al. (2012). Partial MCM4 deficiency in patients with growth retardation, adrenal insufficiency, and natural killer cell deficiency. J Clin Invest 122, 821-832.
15. Hughes, C.R., Guasti, L., Meimaridou, E., Chuang, C.H., Schimenti, J.C., King, P.J., Costigan, C., Clark, A.J., and Metherell, L.A. (2012). MCM4 mutation causes adrenal failure, short stature, and natural killer cell deficiency in humans. J Clin Invest 122, 814-820.
16. Bernard, F., Picard, C., Cormier-Daire, V., Eidenschenk, C., Pinto, G., Bustamante, J.C., Jouanguy, E., Teillac-Hamel, D., Colomb, V., Funck-Brentano, I., et al. (2004). A novel developmental and immunodeficiency syndrome associated with intrauterine growth retardation and a lack of natural killer cells. Pediatrics 113, 136-141.

17. Cottineau, J., Kottemann, M.C., Lach, F.P., Kang, Y.H., Vely, F., Deenick, E.K., Lazarov, T., Gineau, L., Wang, Y., Farina, A., et al. (2017). Inherited GINS1 deficiency underlies growth retardation along with neutropenia and NK cell deficiency. J Clin Invest 127, 1991-2006.
18. Bicknell, L.S., Bongers, E.M., Leitch, A., Brown, S., Schoots, J., Harley, M.E., Aftimos, S., Al-Aama, J.Y., Bober, M., Brown, P.A., et al. (2011). Mutations in the pre-replication complex cause Meier-Gorlin syndrome. Nat Genet 43, 356-359.
19. Bicknell, L.S., Walker, S., Klingseisen, A., Stiff, T., Leitch, A., Kerzendorfer, C., Martin, C.A., Yeyati, P., Al Sanna, N., Bober, M., et al. (2011). Mutations in ORC1, encoding the largest subunit of the origin recognition complex, cause microcephalic primordial dwarfism resembling Meier-Gorlin syndrome. Nat Genet 43, 350-355.
20. Bongers, E.M., Opitz, J.M., Fryer, A., Sarda, P., Hennekam, R.C., Hall, B.D., Superneau, D.W., Harbison, M., Poss, A., van Bokhoven, H., et al. (2001). Meier-Gorlin syndrome: report of eight additional cases and review. Am J Med Genet 102, 115-124.
21. de Munnik, S.A., Bicknell, L.S., Aftimos, S., Al-Aama, J.Y., van Bever, Y., Bober, M.B., Clayton-Smith, J., Edrees, A.Y., Feingold, M., Fryer, A., et al. (2012). Meier-Gorlin syndrome genotype-phenotype studies: 35 individuals with pre-replication complex gene mutations and 10 without molecular diagnosis. Eur J Hum Genet 20, 598-606.
22. Fenwick, A.L., Kliszczak, M., Cooper, F., Murray, J., Sanchez-Pulido, L., Twigg, S.R.F., Goriely, A., McGowan, S.J., Miller, K.A., Taylor, I.B., et al. (2016). Mutations in CDC45, Encoding an Essential Component of the Pre-initiation Complex, Cause Meier-Gorlin Syndrome and Craniosynostosis. American Journal of Human Genetics.
23. Burrage, L.C., Charng, W.L., Eldomery, M.K., Willer, J.R., Davis, E.E., Lugtenberg, D., Zhu, W., Leduc, M.S., Akdemir, Z.C., Azamian, M., et al. (2015). De Novo GMNN Mutations Cause Autosomal-Dominant Primordial Dwarfism Associated with Meier-Gorlin Syndrome. Am J Hum Genet 97, 904-913.
24. Kitao, S., Shimamoto, A., Goto, M., Miller, R.W., Smithson, W.A., Lindor, N.M., and Furuichi, Y. (1999). Mutations in RECQL4 cause a subset of cases of Rothmund-Thomson syndrome. Nat Genet 22, 82-84.
25. Lindor, N.M., Furuichi, Y., Kitao, S., Shimamoto, A., Arndt, C., and Jalal, S. (2000). Rothmund-Thomson syndrome due to RECQ4 helicase mutations: report and clinical and molecular comparisons with Bloom syndrome and Werner syndrome. Am J Med Genet 90, 223-228.
26. Wang, L.L., Levy, M.L., Lewis, R.A., Chintagumpala, M.M., Lev, D., Rogers, M., and Plon, S.E. (2001). Clinical manifestations in a cohort of 41 Rothmund-Thomson syndrome patients. Am J Med Genet 102, 11-17.
27. Van Maldergem, L., Siitonen, H.A., Jalkh, N., Chouery, E., De Roy, M., Delague, V., Muenke, M., Jabs, E.W., Cai, J., Wang, L.L., et al. (2006). Revisiting the craniosynostosis-radial ray hypoplasia association: Baller-Gerold syndrome caused by mutations in the RECQL4 gene. J Med Genet 43, 148-152.
28. Kaariainen, H., Ryoppy, S., and Norio, R. (1989). RAPADILINO syndrome with radial and patellar aplasia/hypoplasia as main manifestations. Am J Med Genet 33, 346-351.
29. Siitonen, H.A., Sotkasiira, J., Biervliet, M., Benmansour, A., Capri, Y., Cormier-Daire, V., Crandall, B., Hannula-Jouppi, K., Hennekam, R., Herzog, D., et al. (2009). The mutation spectrum in RECQL4 diseases. Eur J Hum Genet 17, 151-158.
30. Li, H. (2013). Aligning sequence reads,clone sequences and assembly contigs with BWA-MEM.
31. Faust, G.G., and Hall, I.M. (2014). SAMBLASTER: fast duplicate marking and structural variant read extraction. Bioinformatics 30, 2503-2505.
32. McKenna, A., Hanna, M., Banks, E., Sivachenko, A., Cibulskis, K., Kernytsky, A., Garimella, K., Altshuler, D., Gabriel, S., Daly, M., et al. (2010). The Genome Analysis Toolkit: a MapReduce framework for analyzing next-generation DNA sequencing data. Genome Res 20, 1297-1303.

33. Van der Auwera, G.A., Carneiro, M.O., Hartl, C., Poplin, R., Del Angel, G., Levy-Moonshine, A., Jordan, T., Shakir, K., Roazen, D., Thibault, J., et al. (2013). From FastQ data to high confidence variant calls: the Genome Analysis Toolkit best practices pipeline. Curr Protoc Bioinformatics 43, 11 10 11-33.
34. McLaren, W., Gil, L., Hunt, S.E., Riat, H.S., Ritchie, G.R., Thormann, A., Flicek, P., and Cunningham, F. (2016). The Ensembl Variant Effect Predictor. Genome Biol 17, 122.
35. Lek, M., Karczewski, K.J., Minikel, E.V., Samocha, K.E., Banks, E., Fennell, T., O'Donnell-Luria, A.H., Ware, J.S., Hill, A.J., Cummings, B.B., et al. (2016). Analysis of protein-coding genetic variation in 60,706 humans. Nature 536, 285-291.
36. Martin, C.A., Ahmad, I., Klingseisen, A., Hussain, M.S., Bicknell, L.S., Leitch, A., Nurnberg, G., Toliat, M.R., Murray, J.E., Hunt, D., et al. (2014). Mutations in PLK4, encoding a master regulator of centriole biogenesis, cause microcephaly, growth failure and retinopathy. Nat Genet 46, 1283-1292.
37. Yang, Y., Muzny, D.M., Reid, J.G., Bainbridge, M.N., Willis, A., Ward, P.A., Braxton, A., Beuten, J., Xia, F., Niu, Z., et al. (2013). Clinical whole-exome sequencing for the diagnosis of mendelian disorders. N Engl J Med 369, 1502-1511.
38. Yang, Y., Muzny, D.M., Xia, F., Niu, Z., Person, R., Ding, Y., Ward, P., Braxton, A., Wang, M., Buhay, C., et al. (2014). Molecular findings among patients referred for clinical whole-exome sequencing. JAMA 312, 1870-1879.
39. Singh, G., and Cooper, T.A. (2006). Minigene reporter for identification and analysis of cis elements and trans factors affecting pre-mRNA splicing. Biotechniques 41, 177-181.
40. Bellelli, R., Castellone, M.D., Guida, T., Limongello, R., Dathan, N.A., Merolla, F., Cirafici, A.M., Affuso, A., Masai, H., Costanzo, V., et al. (2014). NCOA4 transcriptional coactivator inhibits activation of DNA replication origins. Mol Cell 55, 123-137.